Nature Environment and Pollution Technology
An International Quarterly Peer-Reviewed Open Access Journal

p-ISSN: 0972-6268 | e-ISSN: 2395-3454 Vol. 25 | No. 4 | Article ID D1878 | 2026

RESEARCH ARTICLE https://doi.org/10.46488/NEPT.2026.v25i04.D1878 OPEN ACCESS

Insights into WRF-Chem Sensitivity in a Coastal Region of Morocco: Chemical Mechanisms, Nesting Options, and Physical Parameterization

Karima Iraoui[1]†, Rachid Moustabchir[1], Hicham Charifi[1], Abdelfettah Benchrif[2] and Ahmed Chirmata[3]
[1]Physics of Environment and Plasmas (PEP), LMER, Faculty of Science, Ibn Zohr University, Agadir, Morocco
[2]Geochemistry and Chemical Pollution Unit (UGPC), National Centre for Nuclear Energy, Science and Technology (CNESTEN), Morocco
[3]Environment Department, Wilaya of Souss Massa Region, Agadir, Morocco
†Corresponding author: Karima Iraoui; karima.iraoui@edu.uiz.ac.ma

ARTICLE HISTORY

Received: 19-09-2025
Revised: 08-11-2025
Accepted: 27-01-2026

KEYWORDS

Modelling performance
Air quality modelling
Sensitivity analysis
Chemical mechanisms
WRF-Chem

CITE THIS ARTICLE

Iraoui, K., Moustabchir, R., Charifi, H., Benchrif, A. and Chirmata, A., 2026. Insights into WRF-Chem sensitivity in a coastal region of Morocco: Chemical mechanisms, nesting options, and physical parameterisation. *Nature Environment and Pollution Technology*, 25(4), D1878. https://doi.org/10.46488/NEPT.2026.v25i04.D1878

PUBLISHED BY

TECHNOSCIENCE PUBLICATIONS

ABSTRACT

The performance of the Weather Research and Forecasting model coupled with chemistry (WRF-Chem) depends on the accuracy of input data and parameterisation schemes. This study examined the sensitivity of WRF-Chem version 4.4.2 to various domain configurations, chemical mechanisms, and physics parameterizations. The model was applied to predict air quality pollutants (PM_{10}, O_3, CO, NO_2, SO_2) and meteorological variables (wind speed and temperature) for the first time over the Moroccan city of Agadir, which features complex topography and land use. Multiple simulations tested the sensitivity of these variables to different chemical mechanisms (MOZART, RACM, GOCART), nesting configurations (three nested domains at a 1:4 ratio and four nested domains at a 1:3 ratio), and planetary boundary layer (PBL) parameterizations (YSU, MYJ, MYNN2, QNSE). The modelled pollutant and meteorological data were then validated against surface observations using various statistical metrics. Results indicated that ozone (O_3) and NO_2 show limited sensitivity to domain configuration and chemical mechanisms, implying they are primarily influenced by local factors, especially emission patterns. Conversely, CO exhibits greater sensitivity to nesting choices due to its dependence on accurately capturing local emissions and atmospheric mixing. Similarly, concentrations of PM_{10}, SO_2, and CO strongly depend on the representation of physical and chemical processes within domain configurations and chemical schemes. Ozone estimates, however, are highly affected by physical parameterizations, particularly those influencing temperature, highlighting the importance of temperature and sunlight in ozone formation. Sensitivity analysis revealed that optimal configurations differ by variable, based on both spatial variation and statistical assessment. For physics parameterizations, the YSU PBL scheme was preferred for predicting wind speed and temperature. Among chemical schemes, GOCART proved most effective for PM_{10}, SO_2, and CO, while MOZART was best suited for O_3 and NO_2. The most efficient nesting setup was identified as three nested domains at a 1:4 ratio, balancing accuracy with computational efficiency. These findings suggest significant potential for improving air quality predictions in the region, though further refinement-particularly for PM_{10}, which exhibited the lowest model accuracy-remains necessary for future research.

1. INTRODUCTION

Air pollution is a pervasive and complex environmental problem that demands careful attention on a global scale. It results from a complex interplay between anthropogenic activities and natural processes that alter the composition of the Earth's atmosphere (World Health Organization 2006). The consequences of air pollution are becoming increasingly significant as humanity continues its trajectory

of industrialization, urbanization, and energy consumption, necessitating extensive investigation supported by robust research (Ciencewicki & Jaspers 2007). Due to rising levels of air pollution, billions of people are at risk of developing health problems (Sicard et al. 2021). Among air pollutants, ground-level ozone (O_3), nitrogen dioxide (NO_2), sulfur dioxide (SO_2), and particulate matter (PM_{10}/$PM_{2.5}$) have the most concerning effects on public health (Bălă et al. 2021, WHO 2003). These pollutants are associated with diseases such as asthma, chronic obstructive pulmonary disease, and cardiovascular disorders (Arghavani et al. 2019, Ciencewicki & Jaspers 2007, Luo et al. 2020). In addition to impairing visibility, air pollution may also retard plant growth and reduce plants' ability to resist certain pathogenic agents. For example, ozone can reduce the agricultural productivity of cereal crops (Arghavani et al. 2019, Manisalidis et al. 2020). For these reasons, it is important to study and forecast the concentrations of these pollutants to reduce their adverse effects on human health, climate, and atmospheric visibility (Lecoeur & Seigneur 2013).

Anthropogenic air pollution emissions significantly affect both the concentration and diversity of chemical components in the atmosphere. However, these emissions represent only one aspect of the factors influencing air quality. Weather conditions also play a significant role. Studies have shown that atmospheric stability, influenced by large-scale weather patterns (synoptic systems) and factors such as wind speed, humidity, and temperature, can substantially affect air quality (Alapaty et al. 2012, Bounakhla et al. 2023). Particulate matter, a major air pollutant, is formed through complex chemical reactions, highlighting the crucial role of atmospheric chemistry in determining air quality (Park 2021a, 2021b, Taşpınar 2015). Additionally, factors including terrain, land use, and other geographical characteristics influence the dispersion of pollutants throughout the environment.

Numerical models are valuable tools for predicting air pollution and understanding the physical and chemical processes involved (Sha et al. 2019). These tools, particularly meteorological models, play a vital role in improving our understanding of how meteorological conditions influence air quality (Liu et al. 2022). The accurate simulation of meteorological variables and chemical species depends on a thorough understanding of local meteorological processes, topography, and pollutant emissions (Misenis & Zhang 2010). Since air pollutants undergo complex chemical reactions in the atmosphere, air quality models combine meteorological forecasts with atmospheric chemistry modelling tools to predict pollution levels (Menut et al. 2021).

Currently, there are two main approaches to analyzing air quality: (i) a qualitative approach based on the study of factors affecting air quality, including industrial activities and societal influences, while considering factors such as population growth, waste incineration, coal combustion, and vehicle exhaust emissions, and (ii) a quantitative approach based on pollutant transport and diffusion mechanisms (Li et al. 2021, Liu et al. 2022). Examples of quantitative approaches include statistical and deterministic models. Statistical methods use historical data to predict the future behavior of various air quality parameters (Qiu et al. 2022). This approach has been widely used for air pollution prediction. For instance, studies have assessed PM□□ and ozone concentrations using conventional statistical methods such as multiple linear regression (MLR) (e.g., Iraoui et al. 2023, Mohammed & Abualqumboz 2018, Mohd Napi et al. 2020, Nazif et al. 2016, Siegfried et al. 2005, Yorkor & Leton 2017), as well as artificial intelligence (AI) techniques, including support vector machines (SVMs), artificial neural networks (ANNs), and deep learning (DL) (Abdul-Wahab & Al-Alawi 2002, Adnane et al. 2020, Bozkurt 2014, Chen et al. 2013, Luna et al. 2014, Park 2021b, Taşpınar 2015, Tebal & Pinang 2011, Wang et al. 2003). While some studies suggest that artificial intelligence methods can achieve higher predictive accuracy, conventional statistical techniques also provide valuable insights. However, statistical models often treat the system as a "black box" and may not explicitly identify the most influential variables. Furthermore, their predictive accuracy depends heavily on the quality and quantity of historical data (Mohan et al. 2011).

Unlike statistical models, deterministic models rely on established principles of chemistry, meteorology, and fluid dynamics. They use mathematical equations to describe how pollutants are transported, transformed, and deposited in the atmosphere, thereby establishing cause-and-effect relationships between the model inputs (initial conditions) and outputs (predictions). Deterministic models are generally classified into two categories: sequential (also known as coupled offline) models and integrated (online) models. Unlike sequential approaches, which treat meteorology and chemistry separately, online models such as WRF-Chem simulate both processes simultaneously. This enables a more comprehensive representation of atmospheric processes, as online models account for the influence of meteorological conditions on the formation, transport, and removal of pollutants. In WRF-Chem, both chemical and meteorological calculations share the same time step and use identical horizontal and vertical grids, facilitating this two-way interaction (Grell et al. 2005).

In recent years, WRF-Chem has become a widely used tool for researchers worldwide. Numerous studies have employed it to simulate both meteorological conditions and air quality using various chemical mechanisms, aerosol schemes, and photolysis options. However, only a limited

number of studies have evaluated WRF-Chem specifically in Morocco and the wider African region, where air quality modelling remains particularly challenging (Ajdour et al. 2020). Table 1 summarizes recent WRF-Chem studies conducted in different parts of the world. These studies highlight limitations in simulating certain air quality parameters, particularly PM_{10} and $PM_{2.5}$. These shortcomings are likely due to uncertainties in the input data and the lack of local emission inventories (Schindlbacher et al. 2021). To reduce discrepancies between modelled and observed pollutant concentrations, previous studies have emphasized the need to investigate the influence of input data sources and model configurations to improve model performance. Accordingly, considerable research has focused on evaluating how WRF-Chem performance varies with different chemical mechanisms, nesting ratios, and physical parameterizations. These studies play a crucial role in understanding how such adjustments influence model accuracy and help determine the optimal WRF-Chem configuration for different applications.

For example, Khan & Kumar (2019) investigated how the initial and boundary conditions for chemical species affect predictions using the MOZART-4 mechanism. Shimada et al. (2011) compared various planetary boundary layer (PBL) schemes within the WRF-ARW model to determine which scheme best reproduces wind speeds over Japan. Yu et al. (2022) evaluated different parameterisation options for the planetary boundary layer (PBL), microphysics (MP), and shortwave/longwave radiation (SW-LW) to identify the WRF model configuration that most accurately simulates wind fields under stable atmospheric conditions in North China. Finally, Cifuentes et al. (2021) analyzed how factors such as lateral chemical boundary conditions (LCBC), domain configurations, nesting options, and chemical mechanisms influence the model's ability to predict CO, O_3, PM_{10}, and $PM_{2.5}$.

Although previous studies have advanced our understanding of air quality modelling, there remains a knowledge gap regarding the optimal chemical mechanism for different regions. The performance of these mechanisms can vary considerably depending on geographical location. This study aims to address this gap by identifying a chemical mechanism that accurately represents air quality conditions in Morocco and North Africa, where such studies remain

Table 1: Summary of WRF-Chem studies reviewed, highlighting geographic focus and key findings.

Study	Model/study area	Study overview
(Kant et al. 2021)	WRF-Chem/India	• In this study, the WRF-Chem numerical model was used to analyse the effects of aerosols on cloud microphysical properties during winter in India in February 2016. The model's performance was assessed for rainfall, aerosol optical depth (AOD), temperature, and wind, showing consistent RMSE, MSE, and MB values in simulations DEF (which deactivated wet filtering and cloud chemistry but activated both aerosol effects) and INDEF (considering indirect aerosol impacts). However, the LCINDEF simulation, which included all INDEF factors with a 50% reduction in anthropogenic emissions, exhibited significant errors.
(Singh et al. 2021)	WRF-Chem/India	• This study analyses an extreme dust episode in India using WRF-Chem, focusing on atmospheric dust dynamics and its impacts on ecosystems and human health. Model evaluation, through categorical validation, indicates a strong correspondence between reanalysis and observational datasets and WRF-Chem's dust load simulations, showing a 0% false alarm rate, a detection likelihood between 78% and 92%, and an accuracy range of 79% to 90%.
(Sicard et al. 2021)	WRF-Chem/ Asian region	• The study evaluates the WRF-Chem model's effectiveness in simulating atmospheric physics and chemistry over Asia. It found that the model accurately approximates spatial distributions of O_3, especially in summer, but significantly underestimates NO_2 concentrations.
(Wang et al. 2020)	WRF-Chem/ Sichuan Basin (China)	• In this study, the WRF-Chem model was utilized to simulate $PM_{2.5}$ and O_3 in the Sichuan Basin of China during January and July 2015. The results indicated that $PM_{2.5}$ levels were accurately modelled for all cities in both months, with mean fractional bias of 0.6 and mean normalized bias of 0.7. Ozone simulation showed good agreement with observational data in July, but concentrations were generally overestimated in January, primarily due to uncertainties in emissions and photochemical processes affecting winter O_3 levels.
(Saidou Chaibou et al. 2019)	WRF-Chem/ North Africa	• This study analyses dust extinction and vertical profiles in North Africa using data from CALIPSO and AERONET, combined with WRF-Chem simulations from the summer of 2006. It aims to enhance understanding of atmospheric dust behavior and its regional impacts. The results indicate that all modelling schemes effectively captured the spatial coherence of total dust emissions. However, differences in threshold friction velocity and soil moisture adjustments led AFWA and UoC schemes to diverge from GOCART regarding extent, magnitude, and patterns, while still showing comparable regional distribution. GOCART displayed good consistency with AFWA and UoC schemes, evidenced by correlation coefficients of 0.5 and 0.8, respectively, despite emitting larger dust flows at times.

limited. To this end, this study uses the WRF-Chem model for the first time to simulate meteorological fields and air quality over Agadir, Morocco. We aim to identify the optimal model configuration by testing different chemical mechanisms, nesting ratios, and physics parameterizations. The resulting configuration will be used for future air quality simulations in Agadir and may also be adapted for other Moroccan cities. This research not only advances air quality modelling in Agadir by employing the more comprehensive WRF-Chem model instead of the previously used WRF-CHIMERE model (e.g., Ajdour et al. 2020, Ajdour 2022), but also establishes a foundation for future research in this field.

The methodology used to assess the performance of the WRF-Chem system and the sensitivity analyses conducted in this study comprises several stages, which are described in the following sections. First, we describe the study area (Morocco, centered on Agadir City) and the model configuration, including the domain size and nesting options. We also describe the datasets used and the physics options selected for the simulations. Next, we present the results of the sensitivity analyses, focusing on how different chemical mechanisms and nesting scenarios affect pollutant concentrations. This analysis helps us understand how these settings influence the model's overall performance. Finally, we summarize the key findings of this investigation and identify the model configurations that have the greatest impact on model performance.

2. MATERIALS AND METHODS

2.1. Description of the Case Study

Agadir is a prominent city located along the southwestern coast of Morocco (Fig. 1). Recently, it has become an area of increasing scientific interest due to its unique geographical and climatic conditions, which influence local air quality (Ajdour et al. 2020, Chirmata et al. 2017). As the capital of the Agadir-Ida Outanane Province and a bustling center for tourism and agriculture (Bouchriti et al. 2023), Agadir experiences a range of air quality issues that reflect both its economic activities and natural environment. The city's location along the Atlantic Ocean and at the foothills of the Atlas Mountains creates distinctive meteorological patterns that influence pollutant dispersion and accumulation (UNECA and UNECE 2014). Following Agadir's reconstruction after the 1960 earthquake, the city experienced rapid urbanization and industrial development. While these developments have boosted the local economy, they have also increased emissions of air pollutants, compounded by pesticide application and fertilizer dust. Additionally, the city's major seaport contributes to air pollution through marine and shipping emissions, further exacerbating the urban air quality situation. Although air quality in other Moroccan cities has received greater research attention, Agadir remains relatively understudied. This lack of information on air quality dynamics in Agadir motivated the present study, which investigates the sensitivity of the WRF-Chem model for this specific region.

2.2. WRF-Chem Model and Setup

WRF-Chem (Weather Research and Forecasting model with Chemistry) is an advanced numerical model designed to integrate atmospheric chemistry with meteorology. The model was developed collaboratively by NOAA, DOE/PNNL, NCAR, and other research institutes (https://www2.acd.ucar.edu/wrf-chem). It simulates the interactions between chemical and meteorological processes to predict air quality under varying atmospheric conditions. The model accounts for both anthropogenic emissions and biogenic sources, enabling detailed investigations of the formation, dispersion, and deposition of pollutants (Grell et al. 2005).

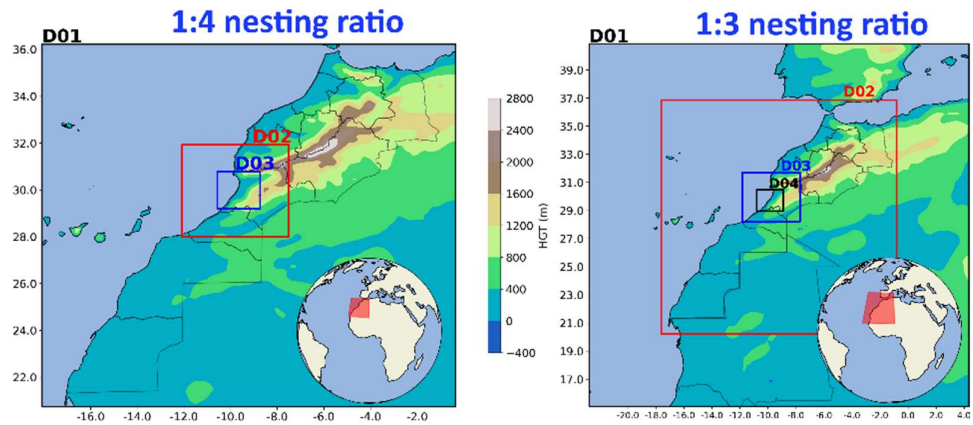

Fig. 1: Study area and domain configuration for nesting ratios of 1:4 (left panel) and 1:3 (right panel).

In this study, WRF-Chem was used to simulate local air quality and atmospheric chemistry. The lateral chemical boundary conditions (LCBC) were based on outputs from the Community Atmosphere Model with Chemistry (CAM-Chem), provided every 6 hours. These outputs supplied comprehensive information on global atmospheric composition, which was essential for initializing and constraining the regional chemical environment. Meteorological boundary conditions were derived from the National Centers for Environmental Prediction (NCEP) Global Forecast System (GFS) data, with a spatial resolution of 0.5˚ × 0.5˚ and a forecast lead time of 3 hours.

The simulation domain was configured using the Mercator projection and included multiple nested domains to achieve progressively finer spatial resolutions. As illustrated in Fig. 1, two domain configurations were employed. The first configuration comprised three nested domains with a 1:4 nesting ratio, in which D01 (the coarsest domain) had a spatial resolution of 16 km, D02 had a resolution of 4 km, and D03 had a resolution of 1 km. The second configuration consisted of four nested domains with a 1:3 nesting ratio, in which D01 had a resolution of 27 km, D02 had a resolution of 9 km, D03 had a resolution of 3 km, and D04 had a resolution of 1 km.

For the 1:3 nesting ratio, the outermost domain (D01) encompassed southern Spain, northern Mauritania, eastern Algeria, and extended westward into the Atlantic Ocean. The second domain (D02) covered the entire Moroccan territory. The innermost domains (D03 and D04) were designated to focus on the study area surrounding Agadir City. A one-way nesting technique was employed for this domain configuration. In this approach, the outermost domain (D01) provided the meteorological data and boundary conditions that drove the simulations within the smaller nested domains, with no feedback from the nested domains to the parent domain. Table 2 summarizes the different model configurations used in this study.

Regarding the emissions data, our study utilized a combination of datasets to accurately represent various emission sources. Due to the absence of a local emission inventory for Agadir, we used the Emission Database for Global Atmospheric Research (EDGAR), which provides a global inventory of anthropogenic emissions at a 1° × 1° horizontal resolution for the year 2010. The EDGAR emissions were spatially interpolated onto the nested WRF-Chem domains using the prep_chem_sources utility, which conserves total mass while redistributing emissions according to the model grid resolution (16 km, 4 km, and 1

Table 2: Setup and sensitivity testing of the WRF-Chem model (version 4.4.2) used in this study.

Model configurations	Options used and sensitivity analysis
Domain	Agadir, Morocco
Domain resolution	3 nested domains (16 km, 4 km, 1 km) 4 nested domains (27 km, 9 km, 3 km, 1 km)
Vertical levels	31 vertical layers
Simulation time	7 days (2–8 May)
Spin-up time	24 h
IC/BC (chemistry)	MOZART global model
IC/BC (meteorology)	NCEP (resolution: 0.5° × 0.5°, 3 h interval)
Biogenic emission inventory	MEGAN
Anthropogenic emission inventory	EDGAR
Microphysics	Morrison double moment
Longwave radiation	RRTMG (Rapid Radiative Transfer Model)
Shortwave radiation	RRTMG (Rapid Radiative Transfer Model)
Surface layer	MM5 similarity based on Monin–Obukhov scheme
Land-surface physics	Noah-MP (multi-physics) land surface model
Planetary boundary layer	Yonsei University scheme Mellor-Yamada-Janjic Quasi-Normal Scale Elimination Mellor-Yamada-Nakanishi-Niino Level 2.5
Chemistry options	Regional Atmospheric Chemistry Mechanism (RACM)/chem_opt=201 Model for Ozone and Related Chemical Tracers (MOZART)/chem_opt=43 Global Oceans Chemistry Aerosol Radiation and Transport (GOCART)/chem_opt=301

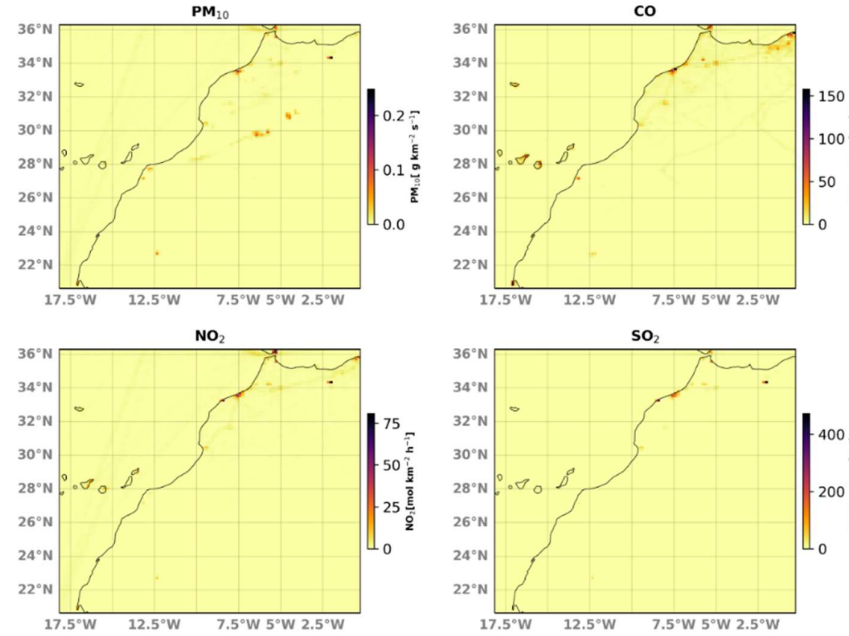

Fig. 2: Spatial pattern of anthropogenic emissions from EDGAR over D01.

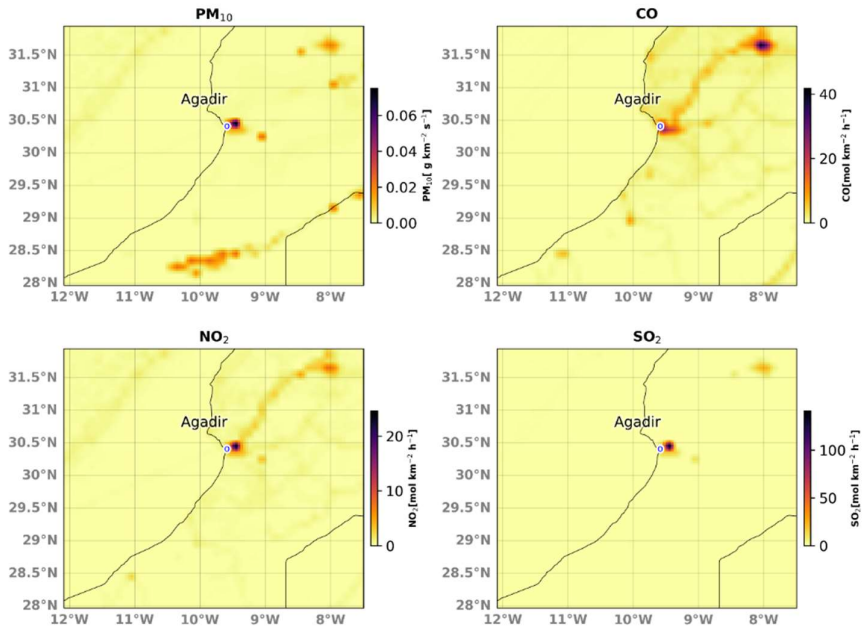

Fig. 3: Spatial pattern of anthropogenic emissions from EDGAR over D02.

km over Agadir). The high-resolution inner domain allowed emissions to be redistributed according to local land-use patterns, road density, and urban extent implicitly represented in the WRF geographical datasets. This framework enabled a detailed representation of anthropogenic emissions across the simulation domains. Figs. 2 and 3 illustrate the spatial distribution of anthropogenic emissions from EDGAR across domains D01 and D02, respectively, for the 1:4 nesting ratio. Biogenic emissions were computed online using the Model of Emissions of Gases and Aerosols from Nature (MEGAN), based on environmental conditions and vegetation types. High-resolution biomass-burning emissions

were incorporated from the Fire Inventory from NCAR (FINNv1.5). The Model for Ozone and Related Chemical Tracers (MOZART-4) was used to provide the initial and lateral boundary conditions (IC/BC) for chemical species in WRF-Chem.

2.3. Sensitivity Runs

To identify the optimal configuration of WRF-Chem version 4.4.2 for predicting air quality variables (carbon monoxide (CO), nitrogen dioxide (NO_2), ozone (O_3), particulate matter (PM_{10}), and sulphur dioxide (SO_2)) and meteorological variables (wind speed (WS) and temperature (T)) over the study area, the model's sensitivity to domain configuration, chemical mechanisms, and physics parameterizations was investigated. This involved a systematic exploration through a series of controlled simulations. Each factor was varied independently to isolate its influence on the accuracy of the model outputs. The procedures followed for these sensitivity tests are illustrated in Fig. 4. The sensitivity of the domain configuration was investigated using different nesting strategies, ranging from broader regional scales to more focused local scales. Specifically, simulations were conducted using both three nested domains (1:4 nesting ratio, 3D) and four nested domains (1:3 nesting ratio, 4D), as described previously.

Three chemical mechanisms were evaluated for their suitability in WRF-Chem simulations. The first mechanism, the Regional Atmospheric Chemistry Mechanism (RACM), includes more than 240 chemical species and 840 reactions, providing a comprehensive representation of atmospheric chemistry (Ha 2022). It was selected because it is a revised version of the Regional Acid Deposition Model, version 2 (RADM2), and provides a more detailed representation of organic chemistry for regional atmospheric pollution modelling. The Model for Ozone and Related Chemical Tracers (MOZART) was also evaluated. This mechanism includes approximately 150 chemical species and more than 300 reactions, providing a more focused representation of atmospheric chemistry (Emmons et al. 2010). It is also consistent with the chemistry used in the global model that provides the chemical boundary conditions for the present simulations. Finally, the Global Ozone Chemistry Aerosol Radiation and Transport (GOCART) mechanism was included in the evaluation. GOCART specializes in simulating complex aerosol interactions, complementing the capabilities of RACM and MOZART (Mian Chin & Lin 2000). The GOCART module simulates the major tropospheric aerosol components, including sulfate, dust, black carbon, organic carbon, and sea salt. It also includes algorithms for dust and sea salt emissions, dry deposition, and gravitational settling. Together, these mechanisms provide detailed representations of atmospheric chemistry across different atmospheric layers and spatial scales, ranging from regional to global.

Regarding the physics schemes, four planetary boundary layer (PBL) parameterisation schemes were evaluated to assess their influence on model performance. The Yonsei University (YSU) scheme was selected because of its non-local closure approach, which is effective for representing vertical transport under convective conditions (Hu et al. 2013). The Mellor-Yamada-Janjic (MYJ) scheme was chosen for its detailed representation of turbulent kinetic energy under both stable and unstable atmospheric conditions (Hu et al. 2010). The Quasi-Normal Scale Elimination (QNSE) scheme was included because of its ability to simulate stable boundary layers by incorporating scale-dependent dynamical processes (Sukoriansky et al. 2006). Finally, the Mellor-Yamada-Nakanishi-Niino Level 2.5 (MYNN2) scheme was selected for its comprehensive representation of boundary layer turbulence and cloud-top cooling effects (Kitamura 2010). This comprehensive sensitivity analysis, encompassing different physics schemes and chemical mechanisms (Fig. 4), was conducted to refine the WRF-Chem model and improve its predictive performance and reliability for air quality modelling in the study region. More details on the physical parameterizations used are available at http://www2.mmm.ucar.edu/wrf/users/phys_references.html

2.4. Datasets for Model Evaluation

During 2010, daily average concentrations of air pollutants and meteorological parameters were collected from a fixed monitoring station located at a school in the city center of Agadir (urban area). The data were provided by the Department of Environment, Wilaya of Agadir, Morocco. The monitored air pollutants included CO, NO_2, O_3, PM_{10}, and SO_2, while the meteorological parameters included temperature (T) and wind speed (WS). Although the availability of observational data limited the analysis to this period, owing to the lack of more recent data, the study still provides valuable insights into air quality trends and their impacts in Agadir. The methodology established in this study can be applied to future datasets as they become available, ensuring the continued relevance and applicability of this research.

2.5. Model Evaluation

The performance of the model was evaluated by comparing the simulated concentrations of air pollutants (PM_{10}, O_3, NO_2, CO, and SO_2) and the simulated meteorological variables (T and WS) with in situ measurements. Several statistical

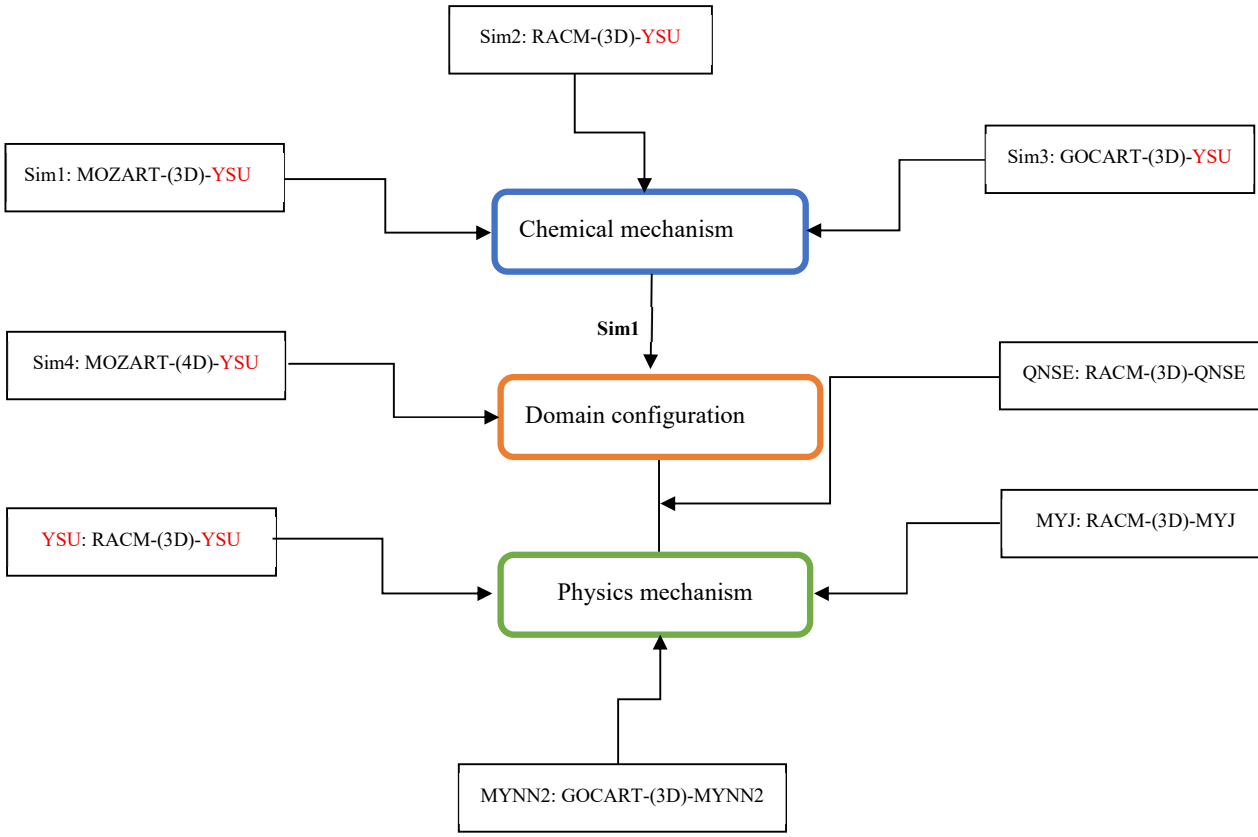

Fig. 4: Flowchart of the research workflow, outlining the specific steps followed in this study to analyse the sensitivity of the WRF-Chem model. **Acronyms: RACM**: Regional Atmospheric Chemistry Mechanism, **MOZART**: Model for Ozone and Related Chemical Tracers, **GOCART**: Global Oceans Chemistry Aerosol Radiation and Transport, **3D**: Three nested domains with a 1:4 nesting ratio, **4D**: Four nested domains with a 1:3 nesting ratio, **YSU: Yonsei University Scheme**, **MYJ**: Mellor-Yamada-Janjic, **QNSE**: Quasi-Normal Scale Elimination, **MYNN2**: Mellor-Yamada-Nakanishi-Niino Level 2.5.

performance metrics were used to assess the model's performance, including Pearson's correlation coefficient (r), mean bias (MB), normalized mean bias (NMB), root mean square error (RMSE), mean absolute gross error (MAGE), and the index of agreement (IOA). These metrics were calculated as follows:

$$r = \frac{\sum_i^n [(O_i - \bar{O})(P_i - \bar{P})]}{\sqrt{\sum_i^n (O_i - \bar{O})^2 * \sum_i^n (P_i - \bar{P})^2}} \quad ...(1)$$

- The correlation coefficient ranges from -1 to 1, with r = 0 indicating no correlation; the strength of the correlation increases as the coefficient approaches -1 or 1.

$$MB = \frac{1}{n}\sum_{i=1}^{n}(P_i - O_i) \quad ...(2)$$

- A positive value of *MB* indicates overestimation of the simulated data, whereas a negative value indicates underestimation. A *MB* value of zero suggests that model predictions are unbiased relative to observations.

$$NMB = \frac{\sum_{i=1}^{n}(P_i - O_i)}{\sum_{i=1}^{n} O_i} \quad ...(3)$$

- A positive *NMB* indicates that predicted variables are higher than observed ones, while a negative *NMB* indicates underprediction. A value of zero implies no bias, indicating ideal model performance.

$$MAGE = \frac{1}{n}\sum_{i=1}^{n}|P_i - O_i| \quad ...(4)$$

- A low value of *MAGE* indicates greater similarity between observed and simulated values.

$$RMSE = \sqrt{\frac{\sum_{i=1}^{n}(P_i - O_i)^2}{n}} \quad ...(5)$$

- A lower value of *RMSE* indicates good agreement between simulated and observed data.

$$IOA = 1 - \frac{\sum_{i=1}^{n}(P_i - O_i)^2}{\sum_{i}^{n}(|P_i - \bar{O}| + |O_i - \bar{O}|)^2} \quad ...(6)$$

- The *IOA* provides a value between 0 and 1, where 1 indicates perfect agreement between model predictions and observed data. A higher *IOA* value indicates a better predictive performance, taking into account both the magnitude and the direction of deviations between the model and observations.

where:

P_i and O_i represent the predicted and observed variables, respectively;

$\bar{P}$ and $\bar{O}$ are the mean values of the predicted and observed values, respectively;

n is the total number of observations used.

3. RESULTS AND DISCUSSION

This section presents the simulation results for air quality variables (PM_{10}, O_3, CO, and NO_2) and meteorological variables (WS and T). Sensitivity analyses were performed using different chemical mechanisms, nesting ratios, and physical parameterizations to identify the most effective WRF-Chem configurations for the study area. These configurations can be recommended for future research. Python was used to analyse the model outputs and calculate the performance metrics. The results of this study are compared with those of a previous WRF-CHIMERE simulation conducted over the same study area and during the same period (Ajdour et al. 2020, Ajdour 2022), using both qualitative (spatial variations) and quantitative (statistical metrics) approaches.

Before a detailed examination of the model sensitivity, the spatial distributions of pollutants are first evaluated. Figs. 5 and 6 depict the average pollutant concentrations simulated over two domains (D01 and D02) using a 1:4 nesting ratio. These Figs. provide the foundation for the sensitivity analysis by establishing the initial pollutant dispersion patterns across the two domains. Such visualizations are essential for understanding the initial conditions and environmental setting, which influence the model's subsequent sensitivity to the different parameters evaluated.

The study area has been identified as having high PM_{10} concentrations due to various pollution sources, including industrial activities, waste incineration, and traffic-related emissions. In 2010, the primary sources of pollution were

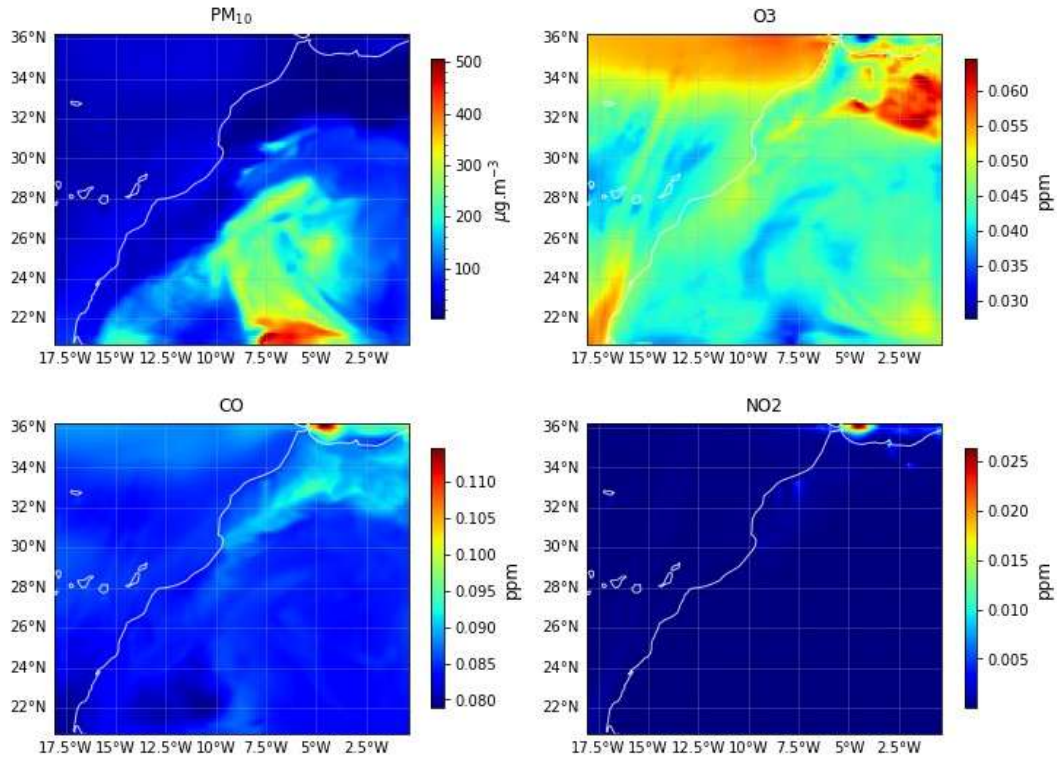

Fig. 5: Average concentration maps for various pollutants across the study domain on May 2, 2010 (D01).

the cement plant, which was still operational at the time, and road traffic (Leghrib et al. 2018). In addition to these sources, the region is affected by the transport of Saharan dust. It should also be noted that the region is located in southern Morocco, making it susceptible to southerly airflow that carries dust storms. These dust storms, in turn, result in elevated PM_{10} concentrations. The Figs. clearly show that PM_{10} concentrations are higher in areas closer to the Sahara, highlighting the influence of geographical and environmental factors on air quality.

3.1. Model Evaluation

3.1.1. Model Evaluation of Meteorological Variables

Table 3 summarizes the performance metrics of WRF-Chem and compares them with those of WRF-CHIMERE for the same case study, with a particular focus on meteorological variables, including wind speed and temperature. The results presented in Table 3 show strong Pearson correlation coefficients (r), ranging from 0.84 to 0.90, for all simulated temperatures, indicating good agreement between the observed and simulated values. All model configurations produced satisfactory results, with RMSE values ranging from 2.5 to 3.0 °C. Furthermore, the temperature mean bias (MB) ranged from 2.12 to 2.77 °C, indicating that the model generally overestimated temperature. Similarly, the wind speed MB ranged from 0.92 to 1.32 m s^{-1}, indicating a consistent overestimation of wind speed. However, for the WRF-Chem configurations, the correlation coefficients for wind speed remained satisfactory, ranging from 0.63 to 0.79, and the RMSE values (0.95–1.53 m s^{-1}) were acceptable and showed an improvement over those reported in the previous WRF-CHIMERE study (Ajdour et al. 2020, Ajdour 2022). Previous studies have reported that both WRF-Chem and WRF-CHIMERE have difficulty accurately simulating wind speed and wind direction (Yu et al. 2022). Therefore, this study sought to improve the physical parameterizations to reduce the bias between the observed and simulated wind speeds, given their critical role in pollutant dispersion.

The simulation results indicate that the predictions of wind speed and temperature are satisfactory. Compared with the previous WRF-CHIMERE study conducted for the same case study, the present study demonstrates improved wind speed simulations. This improvement is clearly illustrated in Fig. 7, which presents the time series of wind speed (WS) and temperature (T) over the simulation period. These improvements are important for more accurately predicting pollutant dispersion, which is strongly influenced by meteorological conditions (Wang & Li 2022).

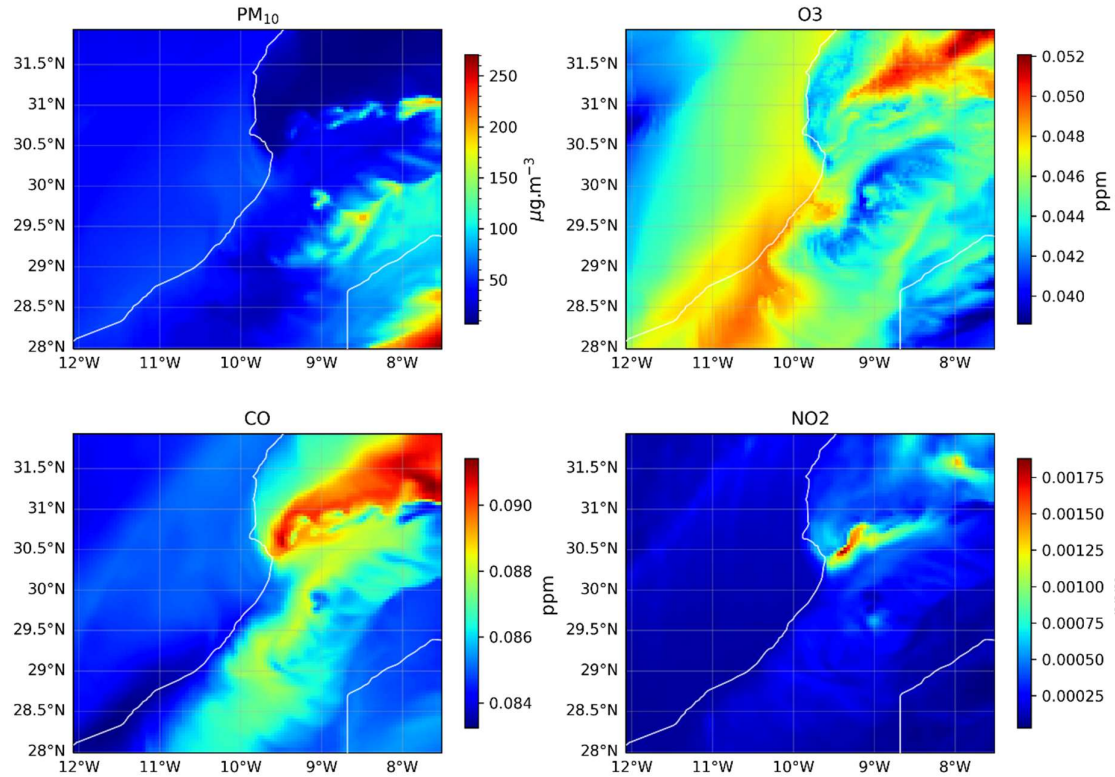

Fig. 6: Average concentration maps for various pollutants across the study domain on May 2, 2010 (D02).

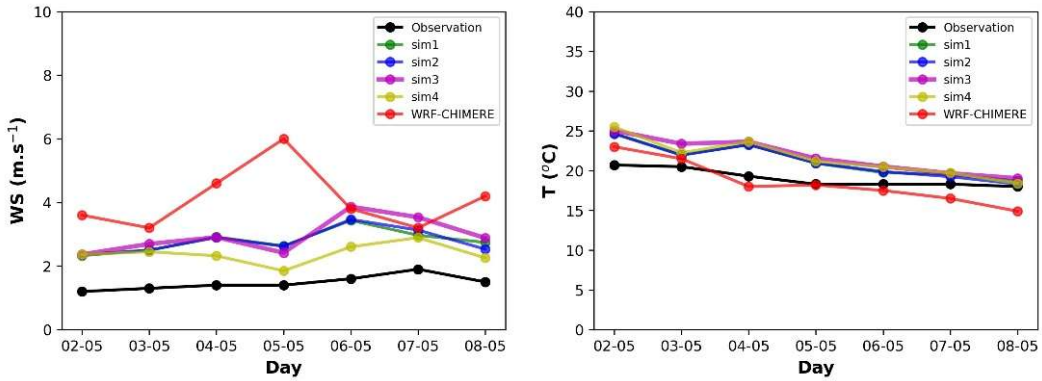

Fig. 7: Time series of daily ground-level wind speed (WS) and temperature (T) during the simulation period from May 2 to May 8.

Table 3: Summary of performance statistics for the sensitivity analyses.

Options	Variable	MB	MAGE	RMSE	NMB	NME	IOA	r
MOZART-(3D)-YSU	T[°C]	2.2	2.2	2.53	11.55	11.55	0.57	0.86
	WS	1.32	1.32	1.34	89.49	89.49	0.23	0.68
	O_3	-1.12	2.14	3.26	-2.04	3.9	0.93	0.92
	CO	2.02	6.65	8.06	10.09	33.25	0.26	-0.13
	NO_2	-15.79	15.79	15.83	-76.75	76.75	0.11	0.38
	PM_{10}	-47.39	47.39	50.23	-72.75	72.75	0.29	-0.13
	SO_2	0.39	1.64	1.98	3.97	16.92	0.37	0.05
RACM-(3D)-YSU	T(°C)	2.12	2.12	2.5	11.11	11.11	0.58	0.84
	WS	1.32	1.32	1.34	89.4	89.4	0.24	0.73
	O_3	8.63	8.63	9.59	15.69	15.69	0.69	0.83
	CO	5.99	7.89	9.46	29.97	39.44	0.46	0.31
	NO_2	-15.37	15.37	15.41	-74.72	74.72	0.11	0.21
	PM_{10}	-39.81	39.81	42.95	-61.12	61.12	0.32	-0.21
	SO_2	1.08	1.29	1.63	11.11	13.24	0.45	-0.01
GOCART-(3D)-YSU	T(°C)	2.53	2.53	2.93	13.28	13.28	0.53	0.84
	WS	0.92	0.92	0.95	62.54	62.54	0.33	0.63
	O_3	-7.95	7.95	8.95	-14.46	14.46	0.64	0.86
	CO	0.42	6.29	7.57	2.08	31.46	0.23	0.1
	NO_2	-15.2	15.2	15.21	-73.9	73.9	0.11	0.91
	PM_{10}	-28.38	28.38	33.85	-43.57	43.57	0.41	0.03
	SO_2	1.53	1.86	2.03	15.72	19.11	0.55	0.52
MOZART-(4D)-YSU	T(°C)	2.77	2.77	3.03	14.56	14.56	0.52	0.9
	WS	1.48	1.48	1.53	100.65	100.65	0.23	0.79
	O_3	-5.7	6.24	7.43	-10.37	11.34	0.75	0.76
	CO	1.97	7.52	8.84	9.87	37.62	0.18	-0.36
	NO_2	-15.9	15.9	15.98	-77.31	77.31	0.1	-0.02
	PM_{10}	-50.03	50.03	52.11	-76.81	76.81	0.28	0.02
	SO_2	-0.96	1.6	1.9	-9.91	16.47	0.49	0.23
WRF-CHIMERE	T(°C)	-0.54	1.49	1.75	-2.85	7.8	0.77	0.94
	WS	2.61	2.61	2.79	177.67	177.67	0.08	-0.22
	O_3	21.29	21.29	21.7	38.7	38.7	0.42	0.81
	CO	102.29	102.29	102.53	511.43	511.43	0.1	0.38
	NO_2	-18.5	18.5	18.53	-89.93	89.93	0.09	-0.22
	PM_{10}	-55.79	55.79	57.33	-85.64	85.64	0.26	-0.09
	SO_2	-7.17	7.17	7.34	-73.82	73.82	0.17	-0.31

3.1.2. Model Evaluation of Air Quality Variables

Table 3 summarizes the statistical metrics obtained from the various simulations of air quality variables, providing detailed insights into model performance across different pollutants. Notably, the O_3 simulations exhibited strong Pearson correlation coefficients, ranging from 0.76 to 0.92, indicating good agreement between the observed and simulated values. For NO_2, the correlation coefficients varied, with generally moderate values (0.21–0.38), except for Sim3 (GOCART-(3D)-YSU), which exhibited a strong correlation coefficient of 0.91. In contrast, the model produced low correlation coefficients for PM_{10} and SO_2, suggesting lower accuracy in simulating these pollutants.

In terms of mean bias (MB), O_3 concentrations were generally underestimated by the model, with one exception (Sim2: RACM-(3D)-YSU), in which O_3 was overestimated. Conversely, PM_{10} and NO_2 were consistently underestimated across all simulations, whereas CO and SO_2 were generally overestimated. These results differ from those obtained with WRF-CHIMERE, which tended to overestimate O_3 and underestimate SO_2. Low RMSE values were obtained for O_3, CO, and SO_2, indicating good model performance for these pollutants. The lowest RMSE values were 3.26 μg m^{-3} for O_3, 8.06 μg m^{-3} for CO, and 1.63 μg m^{-3} for SO_2. In contrast, PM_{10} and NO_2 exhibited higher RMSE values, reaching 42.95 μg m^{-3} and 15.98 μg m^{-3}, respectively.

A comparison with the WRF-CHIMERE performance metrics highlights the improvements achieved in this study:

- **O_3:** O_3 simulations showed substantial improvement. The RMSE decreased from 21.7 μg m^{-3} for WRF-CHIMERE to 3.26 μg m^{-3} in the present study. Similarly, the MB improved from 21.29 μg m^{-3} to −1.12 μg m^{-3}, while the correlation coefficient increased from 0.81 to 0.92. A substantial reduction in the normalized mean error (NME) was also observed, decreasing from 38.7 to 3.9.
- **CO:** The accuracy of CO simulations also improved. The RMSE decreased from 102.53 μg m^{-3} to 7.57 μg m^{-3}, and the MB improved from 102.29 μg m^{-3} to 0.42 μg m^{-3}. The correlation coefficient changed from 0.38 for WRF-CHIMERE to 0.10 for the GOCART-(3D)-YSU simulation.
- **NO_2:** Improvements were also observed for NO_2. The RMSE decreased from 18.53 μg m^{-3} to 15.21 μg m^{-3}, while the MB improved from −18.5 μg m^{-3} to −15.2 μg m^{-3}. The correlation coefficient increased substantially, from −0.22 to 0.91. In addition, the NME decreased from 89.93 to 73.9.
- **PM_{10}:** PM_{10} simulations also improved, with the RMSE decreasing from 57.33 μg m^{-3} for WRF-CHIMERE to 33.86 μg m^{-3}. The MB improved from −55.79 μg m^{-3} to −28.38 μg m^{-3}, although the correlation coefficient remained weak (−0.21 versus 0.09). The NME also decreased from 85.64 to 43.57.
- **SO_2:** Finally, SO_2 simulations showed a substantial improvement. The RMSE decreased from 7.34 μg m^{-3} to 1.63 μg m^{-3}, while the MB improved from −7.17 μg m^{-3} to 0.39 μg m^{-3}. The correlation coefficient increased from −0.31 to 0.52. The NME also improved considerably, decreasing from 73.82 to 13.24.

Overall, these results demonstrate significant improvements in air quality predictions across the study region, particularly for O_3, CO, and SO_2, surpassing the performance achieved by WRF-CHIMERE.

3.2. Chemical Mechanisms Comparison

Fig. 8 illustrates the mean differences in PM_{10}, O_3, CO, and NO_2 concentrations between the MOZART and GOCART chemical mechanisms. This figure provides a comprehensive overview of how each mechanism influences the simulation of different air pollutants. Positive differences indicate regions where MOZART predicts higher concentrations than GOCART, whereas negative differences indicate regions where GOCART predicts higher concentrations than MOZART.

PM_{10} concentrations are particularly sensitive to the choice of chemical mechanism. Across most of the domain, MOZART predicts higher PM_{10} concentrations than GOCART. This can be attributed to MOZART's more detailed treatment of non-methane volatile organic compound (NMVOC) emissions (Emmons et al. 2010) and their conversion into secondary organic aerosols (SOA) (Clappier et al. 2021), which are major components of PM_{10}. An exception is observed in the southeastern Saharan region, where the opposite trend occurs.

For O_3, negative differences predominate, indicating that GOCART generally predicts higher ozone concentrations than MOZART. This is likely due to GOCART's treatment of aerosol interactions, which may influence the scavenging of ozone precursors differently (Kong et al. 2015). Similarly, negative differences are observed throughout the study area for CO, indicating that MOZART predicts lower CO concentrations than GOCART. Finally, the spatial pattern of NO_2 differences closely resembles that of O_3 because of their strong chemical interdependence in urban photochemistry. Consequently, negative NO_2 differences are observed across most of the study area. An exception occurs around Agadir, where MOZART predicts higher NO_2 concentrations because of its more comprehensive treatment of NO_2 emissions and atmospheric lifetimes (Wang et al. 2021).

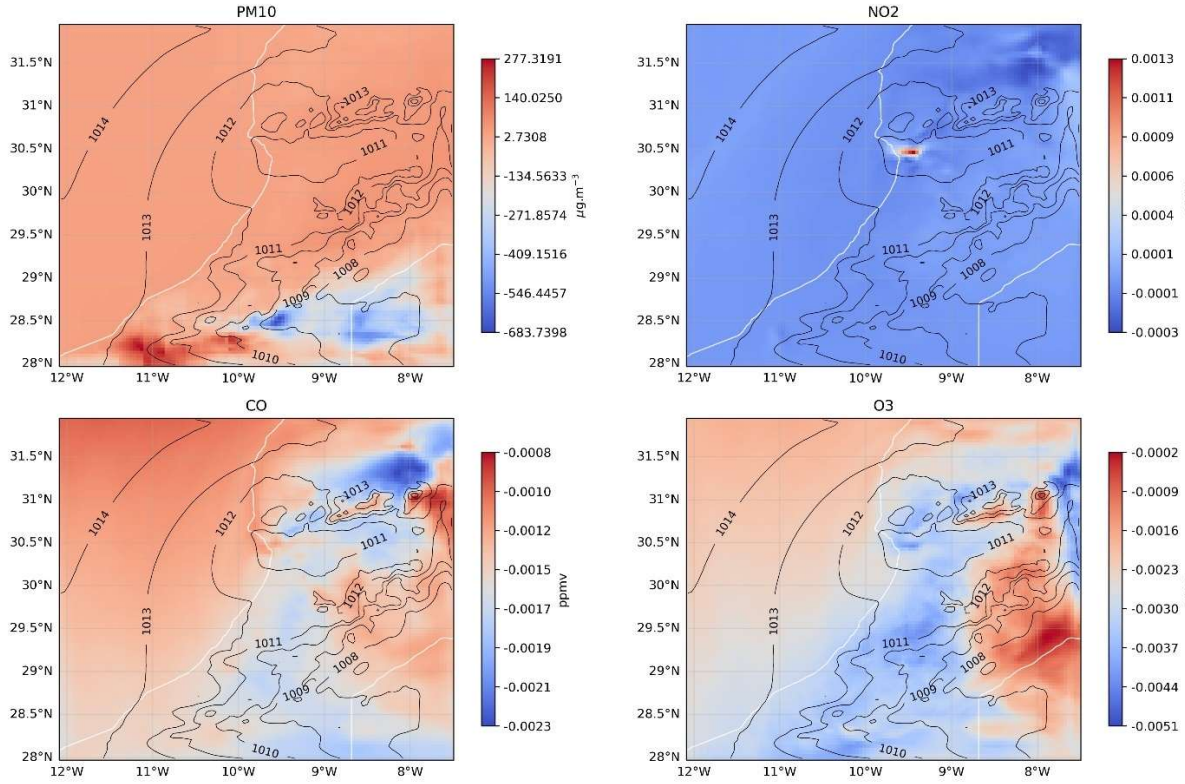

Fig. 8: Mean difference in PM_{10}, NO_2, CO, and O_3 concentrations between MOZART and GOCART.

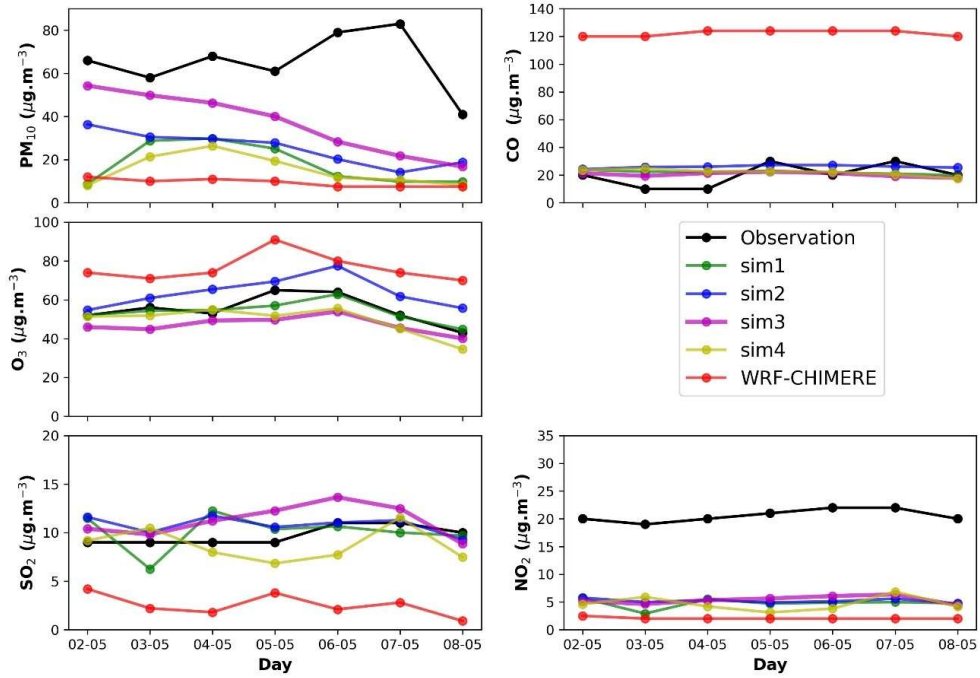

Fig. 9: Time series of daily concentrations of air quality variables (PM_{10}, O_3, SO_2, NO_2 and CO) during the simulation period from May 2 to May 8.

To facilitate comparisons among the different chemical mechanisms, the results of the present study can be compared with those of the previous study shown in Fig. 9. This figure presents time series of air quality variable concentrations simulated using the different chemical mechanisms (Sim1, Sim2, and Sim3). In addition, Figs. 10,

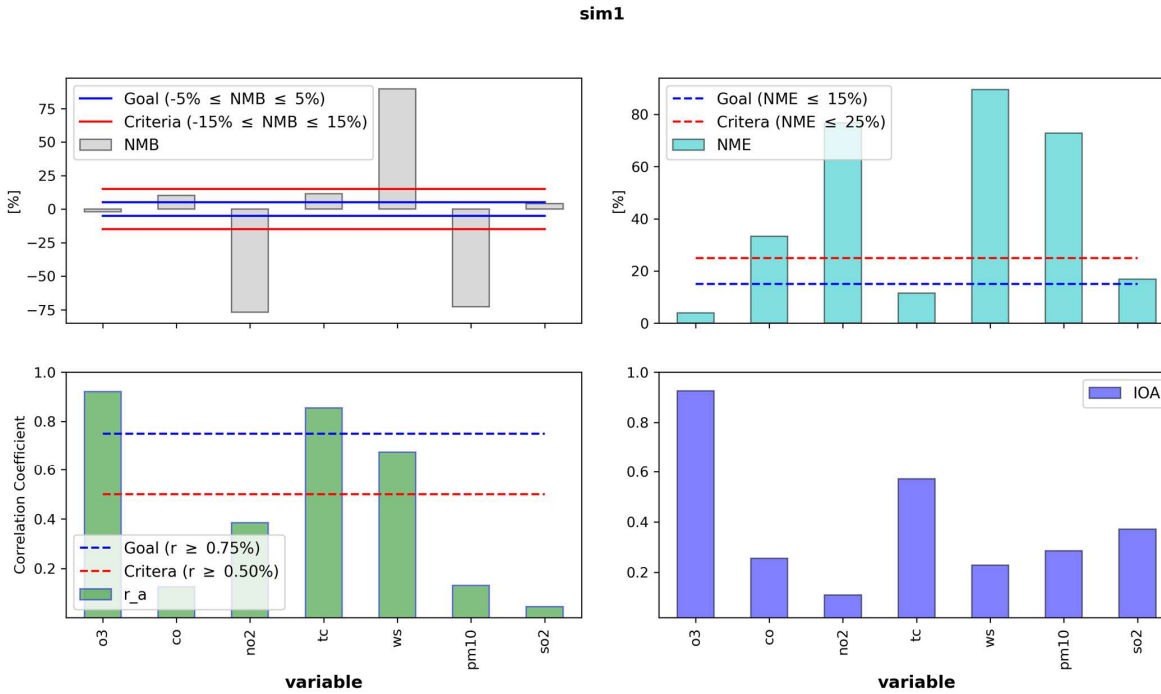

Fig. 10: Statistical plot for the first chemical mechanism, MOZART (simulation 1).

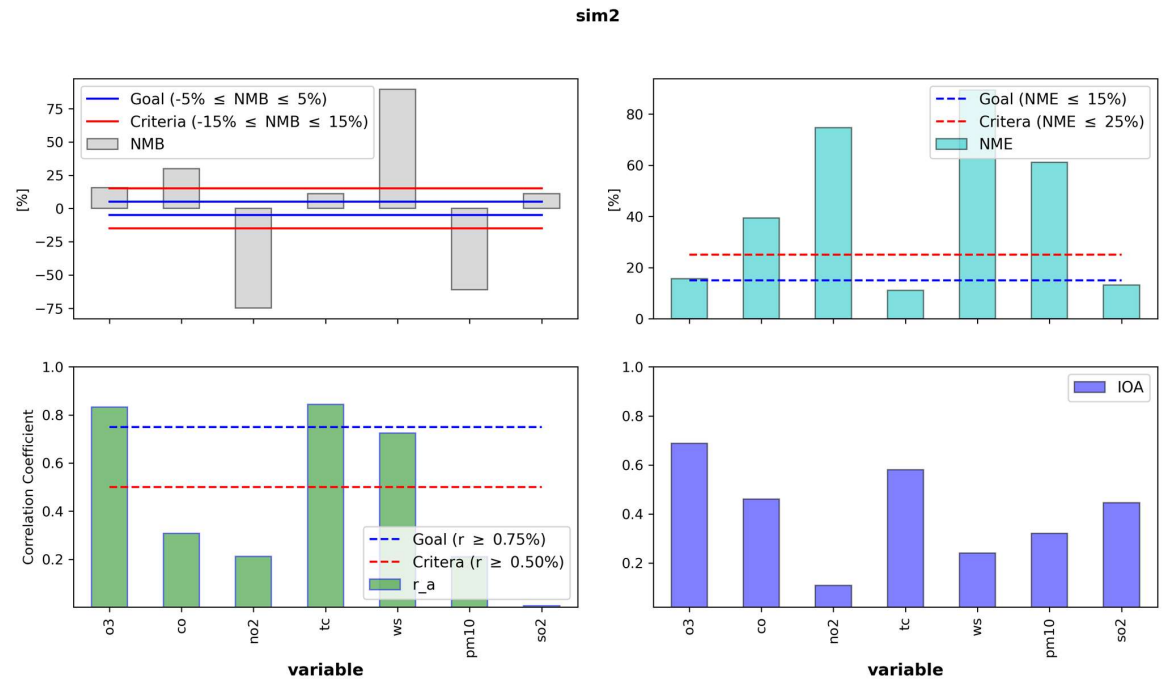

Fig. 11: Statistical plot for the second chemical mechanism, RACM (simulation 2).

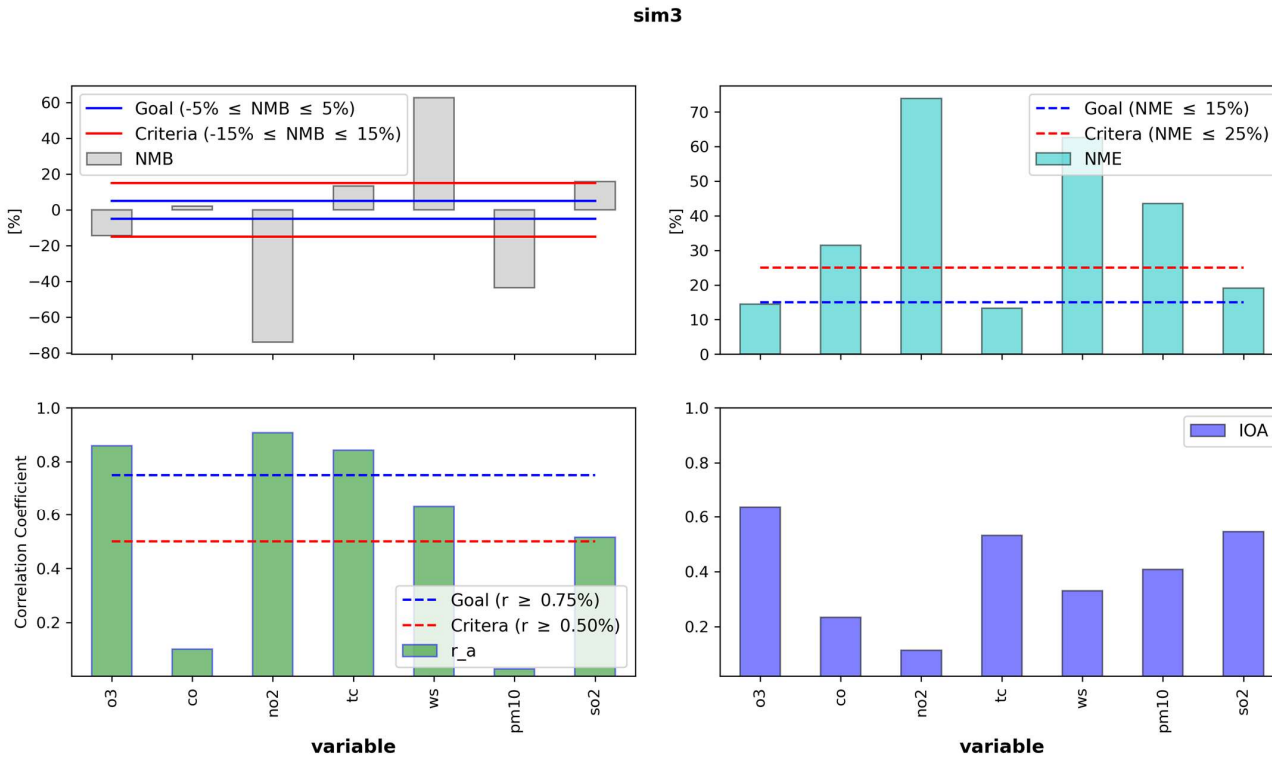

Fig. 12: Statistical plot for the third chemical mechanism, GOCART (simulation 3).

11, and 12 present the principal statistical metrics together with the corresponding statistical performance criteria, enabling the identification of the most suitable chemical mechanism.

Analysis of Fig. 10 shows that, for Sim1 (MOZART), the Pearson correlation coefficient (r) meets the desired criterion (≥ 0.75) for O_3 and temperature and exceeds the acceptable threshold (≥ 0.50) for wind speed (WS). However, it does not satisfy the established criteria for the remaining variables. Similarly, the index of agreement (IOA) for O_3 and temperature is close to 1, while the normalized mean error (NME) is less than or equal to 25%, indicating good model performance in predicting ozone concentrations over the study area.

For Sim2 (RACM), an improvement in the Pearson correlation coefficient (r) is observed for all variables except SO_2 and O_3, for which r decreases (Fig. 11). In the case of Sim3 (GOCART), a substantial improvement in r is observed for NO_2 and SO_2, accompanied by similar improvements in the index of agreement (IOA) (Fig. 12).

Based on these results and the time series shown in Fig. 9, we can conclude that the best chemical mechanism for predicting PM_{10}, SO_2, and CO is GOCART, while the best mechanism for O_3 and NO_2 is MOZART.

3.3. Nesting Ratio Comparison

This section investigates the impact of varying the nesting ratio on simulated meteorological variables (wind speed and temperature) and air quality variables (PM_{10}, CO, NO_2, and O_3). Two nesting configurations were evaluated: one with a 1:4 nesting ratio, in which the nested domain has a spatial resolution four times finer than its parent domain, and another with a 1:3 nesting ratio, in which the nested domain has a spatial resolution three times finer than its parent domain.

3.3.1. Impact of Nesting Ratio on Meteorological Variables

Fig. 13 presents the mean differences in wind speed and temperature between the simulations using three and four nested domains. For wind speed, positive differences predominate, indicating higher values in the three-domain simulation (Sim1) than in the four-domain simulation (Sim4). These differences are most pronounced in high-elevation regions. In contrast, the opposite trend is observed for temperature, except over the Sahara region, where Sim1 predicts higher temperatures, with the differences increasing toward the domain boundaries.

Evaluation of Figs. 10 and 14 show that the four-domain simulation (Sim4) achieves higher Pearson correlation coefficients for both temperature and wind

speed, exceeding the target criterion ($r \geq 0.75$). However, Sim4 also exhibits a higher normalized mean error (NME) for wind speed, exceeding the recommended criterion (NME $\leq$ 25%). Consequently, identifying the optimal nesting ratio for improving the simulation of temperature and wind speed remains challenging. As shown in Fig. 7, the time series of near-surface wind speed and temperature for Sim1 and Sim4 indicate that Sim1 generally produces wind speed values that are closer to the observations. For temperature, however, Sim4 performs better on some days, whereas both simulations produce comparable results on others.

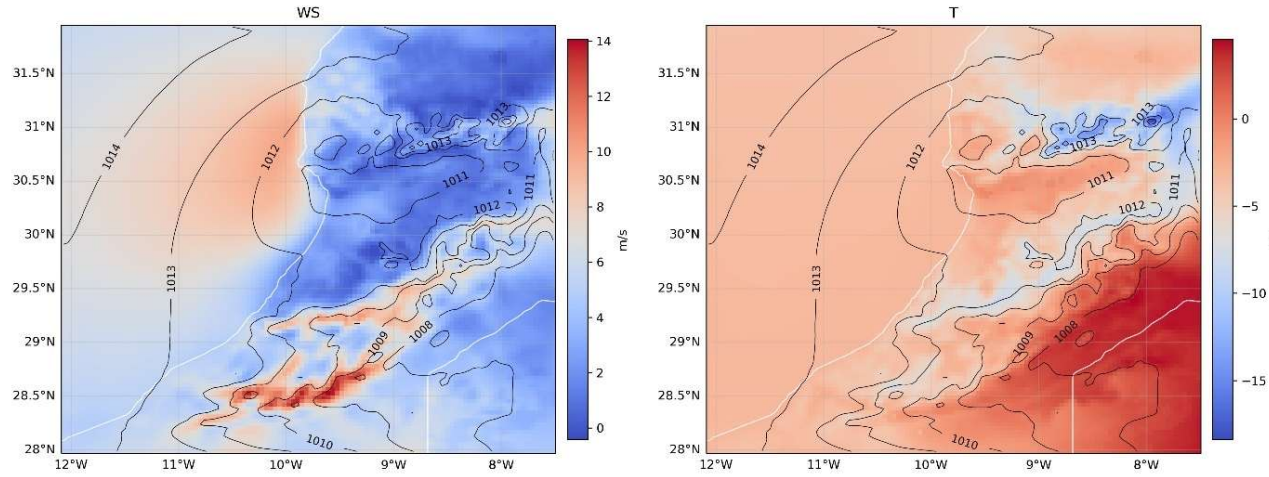

Fig. 13: Mean difference in ground-level WS (left panel) and T (right panel) between 3 nested domains (1:4 nesting ratio) and 4 nested domains (1:3 nesting ratio).

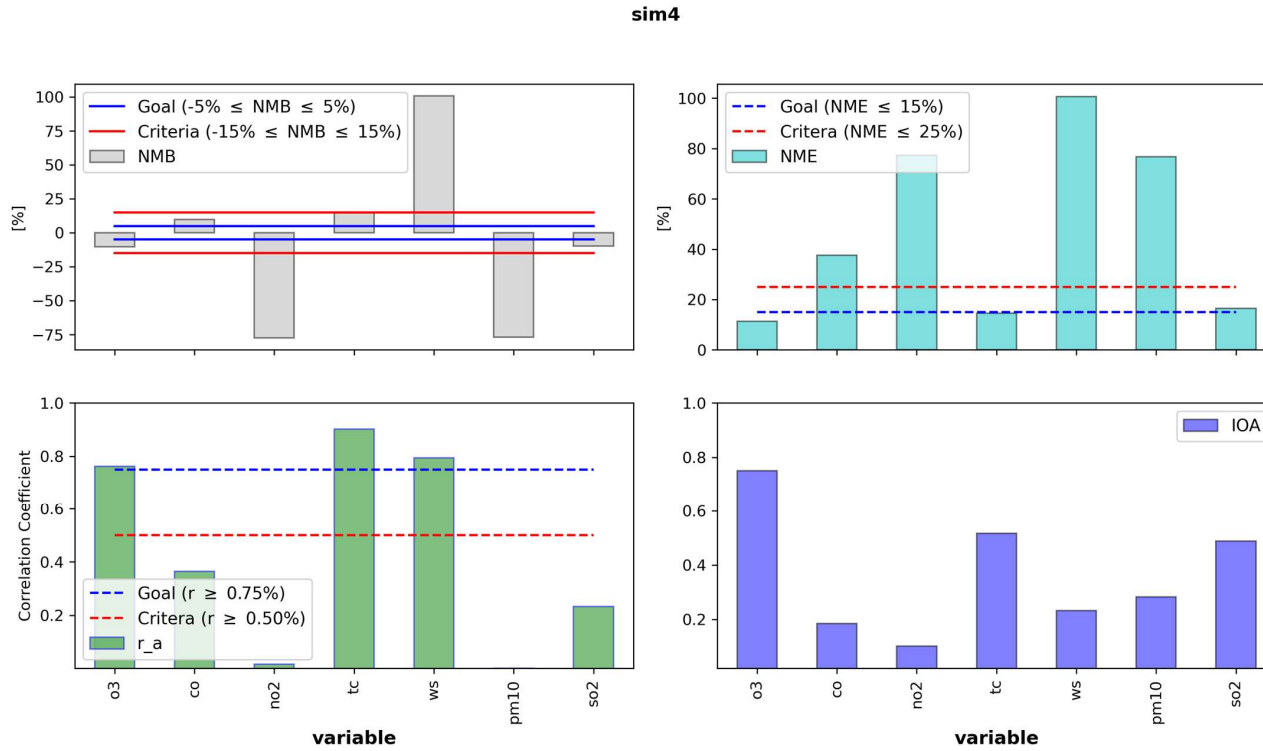

Fig. 14: Statistical plot for the 4 nested domains (1:3 nesting ratio).

Considering these findings, together with the computational cost, which is approximately three times higher for Sim4 than for Sim1, the three-domain configuration with a 1:4 nesting ratio is considered a more effective approach for predicting near-surface temperature and wind speed (Cifuentes et al. 2021).

3.3.2. Impact of Nesting Ratio on Air Quality Variables

Fig. 15 presents the mean differences in PM_{10}, NO_2, CO, and O_3 concentrations between the simulations using three and four nested domains. The figure shows a predominance of positive differences for PM_{10}, indicating that the concentrations predicted by the three-domain configuration are generally higher than those predicted by the four-domain configuration. In contrast, higher concentrations of NO_2, O_3, and CO are predicted by the four-domain configuration.

Analysis of Fig. 14 shows that the four-domain configuration increases the Pearson correlation coefficient (r) for CO from 0.10 to 0.30, while decreasing r for O_3 from 0.90 to 0.79. Similarly, the four-domain configuration results in lower predictive performance for PM_{10} and NO_2. As shown in Fig. 9, the accuracy of the O_3 and PM_{10} simulations is negatively affected when the four-domain configuration is used. For CO and NO_2, both domain configurations exhibit similar performance.

As discussed previously, the four-domain configuration requires substantially greater computational time. Therefore, for air quality prediction in the study region, the three-domain configuration with a 1:4 nesting ratio is recommended, as it provides greater computational efficiency (Cifuentes et al. 2021, Misenis & Zhang 2010).

3.4. Effect of Resolution

Fig. 16 illustrates the impact of model resolution on ozone concentrations. The figure reveals a clear trend: finer spatial resolutions provide greater detail in the simulated ozone concentrations. This suggests that model grid resolution significantly affects the ability to capture and resolve atmospheric processes at finer scales (Tao et al. 2020). Consequently, simulations with higher spatial resolution, such as the four-domain configuration, generally provide more detailed representations of local

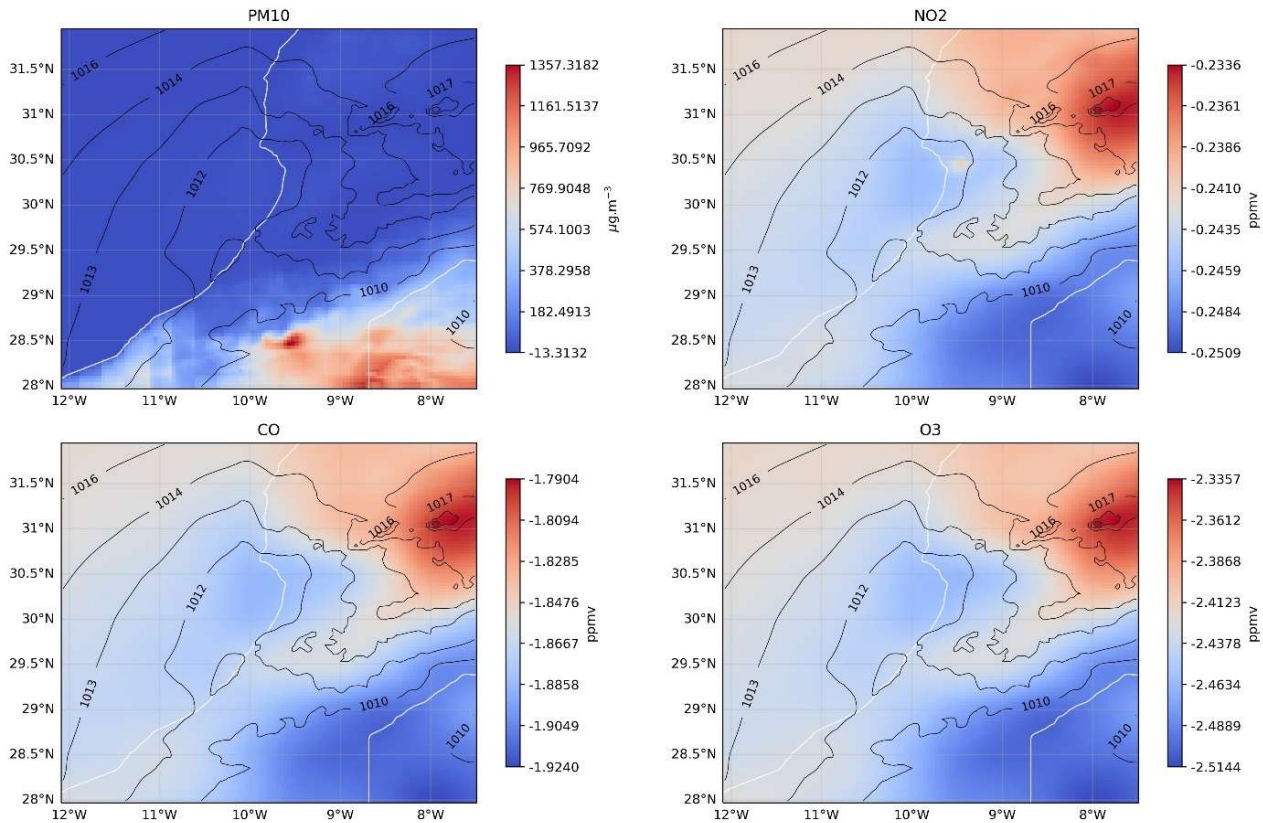

Fig. 15: Mean difference in PM_{10}, NO_2, CO, and O_3 concentrations between 3 nested domains (1:4 nesting ratio) and 4 nested domains (1:3 nesting ratio).

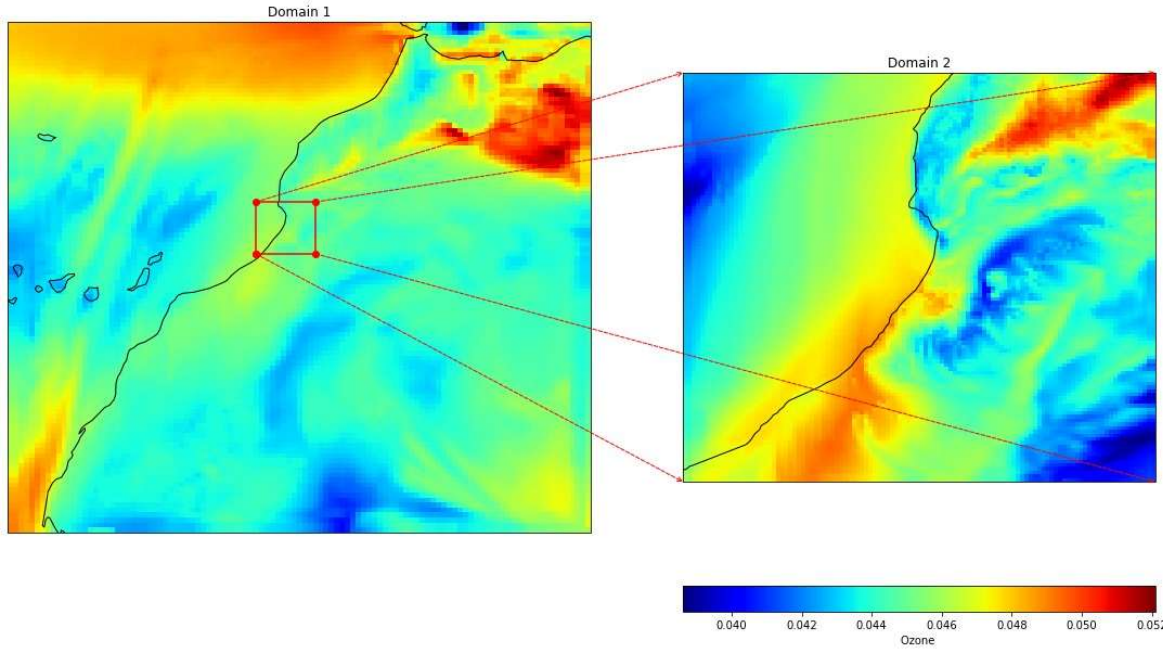

Fig. 16: Plot illustrating the effects of resolution changes between the first domain (D01) and the third one (D03).

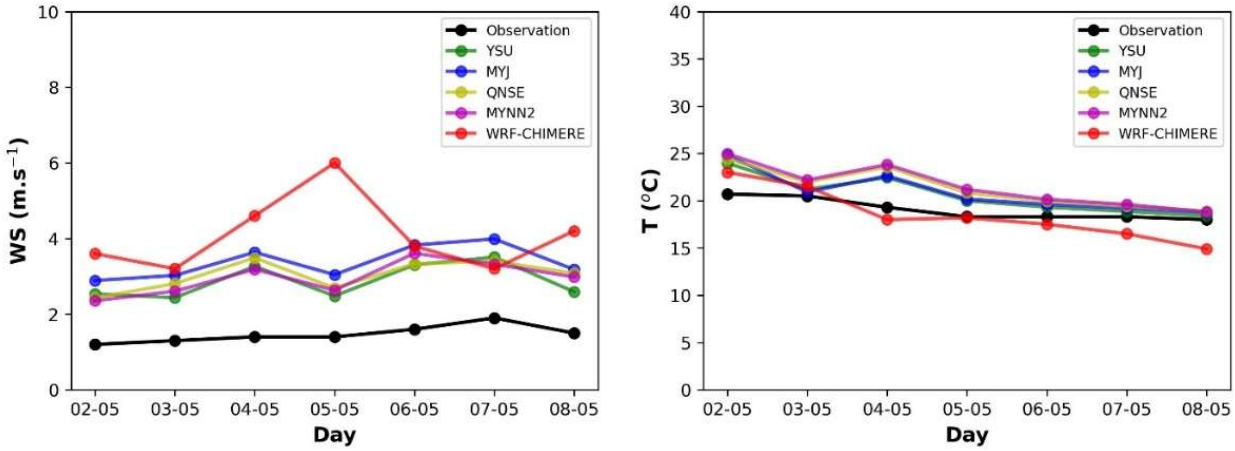

Fig. 17: Time series of daily ground-level wind speed (left panel) and temperature (right panel) during the simulation period from May 2 to May 8, showing the impact of different PBL parameterizations (YSU, MYJ, MYNN2, and QNSE).

phenomena, which is particularly important for air quality and meteorological variables. However, this increased level of detail comes at the expense of greater computational demand. Considering these trade-offs, selecting between the three- and four-domain configurations requires balancing the need for higher spatial resolution against the available computational resources. The three-domain configuration with a 1:4 nesting ratio offers greater computational efficiency, making it a more suitable option for studies with significant time and resource constraints (Misenis & Zhang 2010).

3.5. Impacts of PBL Parameterizations on Meteorological Variables

The selection of a planetary boundary layer (PBL) parameterisation scheme has a significant impact on the simulation of meteorological variables. Fig. 17 compares the performance of the different PBL schemes, including YSU, MYJ, MYNN2, and QNSE. Analysis of wind speed (WS) and temperature (T) indicates that the YSU scheme provides the best performance for predicting near-surface wind speed. Similarly, for temperature, the YSU scheme demonstrates

the best overall performance, followed closely by the MYJ scheme. These findings underscore the importance of selecting an appropriate PBL parameterisation to improve the accuracy of meteorological simulations (Banks & Baldasano 2016, Rizza et al. 2020), particularly for variables such as wind speed and temperature, which directly influence a wide range of atmospheric applications (Misenis & Zhang 2010).

4. CONCLUSIONS

This study successfully implemented the WRF-Chem model over the Moroccan domain for the first time. The model was used to simulate both meteorological variables (WS and T) and air quality variables (PM_{10}, O_3, CO, NO_2, and SO_2). The sensitivity of the model to different configurations was also evaluated. This included testing two nesting configurations (three nested domains with a 1:4 nesting ratio and four nested domains with a 1:3 nesting ratio), examining the effects of three chemical mechanisms (MOZART, RACM, and GOCART), and evaluating four planetary boundary layer (PBL) schemes (YSU, MYJ, MYNN2, and QNSE) to identify the optimal model configuration.

The simulated meteorological and air quality variables were compared with observations and with the results of a previous study conducted over Agadir using WRF-CHIMERE. Statistical performance metrics were calculated for the same study period to facilitate comparison. Overall, the results demonstrate improved air quality predictions over the study area compared with those obtained using WRF-CHIMERE.

The sensitivity analysis revealed satisfactory biases and correlation coefficients that are consistent with those reported in previous studies. Model performance was found to be case-dependent, with the optimal configuration varying according to the variable of interest. For simulations focusing on ozone and nitrogen dioxide, MOZART was identified as the most suitable chemical mechanism, whereas GOCART produced the best results for PM_{10}, SO_2, and CO. The three-domain configuration with a 1:4 nesting ratio was identified as the optimal nesting strategy, providing a 15% reduction in computational time compared with the 1:3 nesting ratio. In addition, the YSU scheme was identified as the optimal PBL parameterisation for improving the simulation of wind speed and temperature.

Despite these improvements, the model performance, particularly for PM_{10}, NO_2, and wind speed (WS), remains below the desired level. Wind speed is a critical factor influencing pollutant transport and air quality distribution, especially in coastal regions such as Agadir, where sea- and land-breeze circulations strongly influence local meteorological conditions. The study is also constrained by the limited availability of observational data, relying on measurements from a single monitoring station collected in 2010, as well as by the absence of high-resolution local emission inventories, both of which may contribute to the underestimation of urban-scale pollutants. Furthermore, although the MOZART, RACM, and GOCART schemes represent key chemical and aerosol processes, simplifications in secondary aerosol formation and heterogeneous reactions limit the accuracy of PM predictions. Despite these limitations, the results provide a valuable benchmark for future studies and highlight the importance of improving local emission inventories, expanding observational networks, and refining model configurations to better represent air quality processes in Morocco.

5. ACKNOWLEDGMENTS

The authors acknowledge with gratitude the cooperation and support of the Wilaya and the Region of Souss Massa in conducting this research. Special thanks are extended to the Wali and the President of the Region for their valuable guidance. This study was carried out with the support of the CNRST Morocco.

6. REFERENCES

Abdul-Wahab, S.A. and Al-Alawi, S.M., 2002. Assessment and prediction of tropospheric ozone concentration levels using artificial neural networks. *Environmental Modelling and Software*, 17(3), pp.219-228. [DOI]

Adnane, A., Leghrib, R. and Chaoufi, J., 2020. The use of a recurrent neural network for forecasting ozone concentrations in the city of Agadir (Morocco). *Journal of Atomic, Molecular, Condensed Matter and Nano Physics*, 7(3), pp.197-206. [DOI]

Ajdour, A., Leghrib, R., Chaoufi, J., Fetmaoui, H., Bousseta, M. and Chirmata, A., 2020. Assessment of particulate matter (PM) using chemistry transport modeling in Agadir City, Morocco. *Journal of Atomic, Molecular, Condensed Matter and Nano Physics*, 7(3), pp.231-240. [DOI]

Ajdour, A., 2022. Surveillance and modelling of urban air pollution in Morocco: case of the cities of Agadir and Casablanca. PhD Thesis. Faculty of Science. Ibn Zohr University.

Alapaty, K., Mathur, R., Pleim, J., Hogrefe, C., Rao, S.T., Ramaswamy, V., Galmarini, S., Schaap, M., Makar, P., Vautard, R., Baklanov, A., Kallos, G., Vogel, B. and Sokhi, R., 2012. New directions: understanding interactions of air quality and climate change at regional scales. *Atmospheric Environment*, 49, pp.419-421. [DOI]

Arghavani, S., Malakooti, H. and Bidokhti, A.A., 2019. Numerical evaluation of urban green space scenarios effects on gaseous air pollutants in Tehran Metropolis based on WRF-Chem model. *Atmospheric Environment*, 214, p.116832. [DOI]

Bălă, G.P., Râjnoveanu, R.M., Tudorache, E., Motișan, R. and Oancea, C., 2021. Air pollution exposure—the (in)visible risk factor for respiratory diseases. *Environmental Science and Pollution Research*, 28(16). [DOI]

Banks, R.F. and Baldasano, J.M., 2016. Impact of WRF model PBL schemes on air quality simulations over Catalonia, Spain. *The Science of the Total Environment*, 572, pp.98-113. [DOI]

Bouchriti, Y., Korrida, A., Ait Haddou, M., Achbani, A., Sine, H., Rida, J., Sine, H., Amiha, R. and Kabbachi, B., 2023. Assessment of health

impact of the surface ozone on a population residing at Agadir city (Morocco) using the AirQ+ model. *E3S Web of Conferences*, 364, pp.0-5. [DOI]

Bounakhla, Y., Benchrif, A., Costabile, F., Tahri, M., Gourch, B.E., Kafssaoui, E., Hassan, E., Zahry, F. and Bounakhla, M., 2023. Overview of PM10, PM2.5 and BC and their dependent relationships with meteorological variables in an urban area in northwestern Morocco. *Journal of Environmental Science and Health, Part A*, 58(4), pp.301-315.

Bozkurt, Z., 2014. Prediction of daily maximum PM10 concentration in Düzce, Turkey: Application of artificial neural networks and regression models in the prediction of daily maximum PM10 concentration in Düzce, Turkey. *Journal of Environmental Protection and Ecology*, 15(1), pp.60-75.

Chen, Y., Shi, R., Shu, S. and Gao, W., 2013. Ensemble and enhanced PM 10 concentration forecast model based on stepwise regression and wavelet analysis. *Atmospheric Environment*, 74, pp.346-359. [DOI]

Chirmata, A., Leghrib, R. and Ichou, I.A., 2017. Implementation of the air quality monitoring network at Agadir City in Morocco. *Journal of Environmental Protection*, 8(4), pp.540-567. [DOI]

Ciencewicki, J. and Jaspers, I., 2007. Air pollution and respiratory viral infection. *Inhalation Toxicology*, 19(14), pp.1135-1146. [DOI]

Cifuentes, F., González, C.M. and Aristizábal, B.H., 2021. Insights to WRF-Chem sensitivity in a zone of complex terrain in the tropical Andes: effect of boundary conditions, chemical mechanisms, nesting, and domain configuration. *Atmospheric Pollution Research*, 12(6), p.101093. [DOI]

Clappier, A., Belis, C.A., Pernigotti, D. and Thunis, P., 2021. Source apportionment and sensitivity analysis: two methodologies with two different purposes. *Environmental Modelling & Software*, 145, p.105201.

Emmons, L.K., Walters, S., Hess, P.G., Lamarque, J.F., Pfister, G.G., Fillmore, D., Granier, C., Guenther, A., Kinnison, D., Laepple, T., Orlando, J., Tie, X., Tyndall, G., Wiedinmyer, C., Baughcum, S.L. and Kloster, S., 2010. Description and evaluation of the model for ozone and related chemical tracers, version 4 (MOZART-4). *Geoscientific Model Development*, 3(1), pp.43-67. [DOI]

Grell, G.A., Peckham, S.E., Schmitz, R., McKeen, S.A., Frost, G., Skamarock, W.C. and Eder, B., 2005. Fully coupled "online" chemistry within the WRF model. *Atmospheric Environment*, 39(37), pp.6957-6975. [DOI]

Ha, S., 2022. Implementation of aerosol data assimilation in WRFDA (v4.0.3) for WRF-Chem (v3.9.1) using the RACM/MADE-VBS scheme. *Geoscientific Model Development*, 15(4), pp.1769-1788. [DOI]

Hu, X.M., Klein, P.M. and Xue, M., 2013. Evaluation of the updated YSU planetary boundary layer scheme within WRF for wind resource and air quality assessments. *Journal of Geophysical Research: Atmospheres*, 118(18), pp.10,490-10,505. [DOI]

Hu, X.M., Nielsen-Gammon, J.W. and Zhang, F., 2010. Evaluation of three planetary boundary layer schemes in the WRF model. *Journal of Applied Meteorology and Climatology*, 49(9), pp.1831-1844. [DOI]

Iraoui, K., Moustabchir, R., Charifi, H., Ouattab, M. and Chirmata, A., 2023. Ozone concentrations predicting in Agadir city (Morocco) using the multiple linear regression (forward regression analysis). In: *2023 3rd International Conference on Innovative Research in Applied Science, Engineering and Technology (IRASET)*, pp.1-4. [DOI]

Kant, S., Panda, J., Rao, P., Sarangi, C. and Ghude, S.D., 2021. Study of aerosol-cloud-precipitation-meteorology interaction during a distinct weather event over the Indian region using WRF-Chem. *Atmospheric Research*, 247, p.105144. [DOI]

Khan, A.W. and Kumar, P., 2019. Impact of chemical initial and lateral boundary conditions on air quality prediction. *Advances in Space Research*, 64(6), pp.1331-1342. [DOI]

Kitamura, Y., 2010. Modifications to the Mellor-Yamada-Nakanishi-Niino (MYNN) model for the stable stratification case. *Journal of the Meteorological Society of Japan*, 88(5), pp.857-864. [DOI]

Kong, X., Forkel, R., Sokhi, R.S., Suppan, P., Baklanov, A., Gauss, M., Brunner, D., Barò, R., Balzarini, A., Chemel, C., Curci, G., Jiménez-Guerrero, P., Hirtl, M., Honzak, L., Im, U., Pérez, J.L., Pirovano, G., San Jose, R., Schlünzen, K.H. and Galmarini, S., 2015. Analysis of meteorology-chemistry interactions during air pollution episodes using online coupled models within AQMEII phase-2. *Atmospheric Environment*, 115, pp.527-540. [DOI]

Lecoeur, E. and Seigneur, C., 2013. Dynamic evaluation of a multi-year model simulation of particulate matter concentrations over Europe. *Atmospheric Chemistry and Physics*, 13(8), pp.4319-4337. [DOI]

Leghrib, R., Ajdour, A., Chirmata, A., Chaoufi, J., Kaaya, A., Fatmaoui, H., Ichou, I.A., Menut, L. and Mailler, S., 2018. Particulate matter monitoring in Souss Massa Region. *SMETox Journal*, 1(4), pp.128-136.

Li, X., Hussain, S.A., Sobri, S. and Md Said, M.S., 2021. Overviewing the air quality models on air pollution in Sichuan Basin, China. *Chemosphere*, 271, p.129502. [DOI]

Liu, Y., Wang, P., Li, Y., Wen, L. and Deng, X., 2022. Air quality prediction models based on meteorological factors and real-time data of industrial waste gas. *Scientific Reports*, 12(1), pp.1-15. [DOI]

Luna, A.S., Paredes, M.L.L., de Oliveira, G.C.G. and Corrêa, S.M., 2014. Prediction of ozone concentration in tropospheric levels using artificial neural networks and support vector machine at Rio de Janeiro, Brazil. *Atmospheric Environment*, 98, pp.98-104. [DOI]

Luo, C., Wang, W., Sheng, L., Zhou, Y., Hu, Z., Qu, W., Li, X. and Hai, S., 2020. Influence of polluted dust on chlorophyll-a concentration and particulate organic carbon in the subarctic North Pacific Ocean based on satellite observation and the WRF-Chem simulation. *Atmospheric Research*, 236, p.104812. [DOI]

Manisalidis, I., Stavropoulou, E., Stavropoulos, A. and Bezirtzoglou, E., 2020. Environmental and health impacts of air pollution: a review. *Frontiers in Public Health*, 8, pp.1-13. [DOI]

Menut, L., Bessagnet, B., Khvorostiyanov, D., Monge, J., Valari, M. and Vautard, R., 2021. Tropospheric ozone and particulate matter modelling. *Atmospheric Chemistry and Physics*, 21(5), pp.4123-4150.

Mian Chin, R.B.R. and Lin, S.-J., 2000. Atmospheric sulfur cycle. *Journal of Geophysical Research: Atmospheres*, 105(D20), pp.24667-24683. [DOI]

Misenis, C. and Zhang, Y., 2010. An examination of sensitivity of WRF/Chem predictions to physical parameterizations, horizontal grid spacing, and nesting options. *Atmospheric Research*, 97(3), pp.315-334. [DOI]

Mohammed, A.N.N.I. and Abualqumboz, A.M.M.S., 2018. Multivariate analysis of monsoon seasonal variation and prediction of particulate matter episode using regression and hybrid models. *International Journal of Environmental Science and Technology*, 16(3), pp.1453-1468. [DOI]

Mohan, M., Kandya, A. and Yadav, M., 2011. An evaluation and comparison of the various statistical and deterministic techniques for forecasting the concentration of criteria air pollutants. *International Journal of Environment and Pollution*, 44(1-4), pp.96-105. [DOI]

Mohd Napi, N.N.L., Noor Mohamed, M.S., Abdullah, S., Mansor, A.A., Ahmed, A.N. and Ismail, M., 2020. Multiple linear regression (MLR) and principal component regression (PCR) for ozone (O3) concentrations prediction. *IOP Conference Series: Earth and Environmental Science*, 616(1), p.012004. [DOI]

Nazif, A., Mohammed, N.I., Malakahmad, A. and Abualqumboz, M.S., 2016. Application of step wise regression analysis in predicting future particulate matter concentration episode. *Water, Air, and Soil Pollution*, 227(4), p.117. [DOI]

Park, J., 2021a. A particulate matter concentration prediction model based on long short-term memory and an artificial neural network. *International*

Journal of Environmental Research and Public Health, 18(13), p.6801. [DOI]

Park, J. and Chang, S., 2021b. A particulate matter concentration prediction model based on long short-term memory and an artificial neural network. *International Journal of Environmental Research and Public Health*, 18(13), p.6801. [DOI]

Qiu, M., Zigler, C. and Selin, N.E., 2022. Statistical and machine learning methods for evaluating trends in air quality under changing meteorological conditions. *Atmospheric Chemistry and Physics*, 22(16), pp.10551-10566. [DOI]

WHO 2003. Health aspects of air pollution with particulate matter, ozone and nitrogen dioxide. *WHO Regional Office for Europe*, pp.1-89.

Rizza, U., Mancinelli, E., Canepa, E., Piazzola, J., Missamou, T., Yohia, C., Morichetti, M., Virgili, S., Passerini, G. and Miglietta, M.M., 2020. WRF sensitivity analysis in wind and temperature fields simulation for the northern Sahara and the Mediterranean Basin. *Atmosphere*, 11(3), p.259. [DOI]

Saidou Chaibou, A.A., Ma, X., Kumar, K.R., Jia, H., Tang, Y. and Sha, T., 2019. Evaluation of dust extinction and vertical profiles simulated by WRF-Chem with CALIPSO and AERONET over North Africa. *Journal of Atmospheric and Solar-Terrestrial Physics*, 199, p.105213. [DOI]

Schindlbacher, S., Matthews, B. and Ullrich, B., 2021. Uncertainties and recalculations of emission inventories submitted under CLRTAP. *CEIP Report*, pp.1-26.

Sha, T., Ma, X., Jia, H., Tian, R., Chang, Y., Cao, F. and Zhang, Y., 2019. Aerosol chemical component: simulations with WRF-Chem and comparison with observations in Nanjing. *Atmospheric Environment*, 218, p.116982. [DOI]

Shimada, S., Ohsawa, T., Chikaoka, S. and Kozai, K., 2011. Accuracy of the wind speed profile in the lower PBL as simulated by the WRF model. *Scientific Online Letters on the Atmosphere*, 7(1), pp.109-112. [DOI]

Sicard, P., Crippa, P., De Marco, A., Castruccio, S., Giani, P., Cuesta, J., Paoletti, E., Feng, Z. and Anav, A., 2021. High spatial resolution WRF-Chem model over Asia: physics and chemistry evaluation. *Atmospheric Environment*, 244, p.118004. [DOI]

Siegfried, H., Pfeiler, B. and Stadlober, E., 2005. Analysis and prediction of particulate matter PM10 for the winter season in Graz. *Austrian Journal of Statistics*, 34(4), pp.307-326.

Singh, C., Singh, S.K., Chauhan, P. and Budakoti, S., 2021. Simulation of an extreme dust episode using WRF-CHEM based on optimal ensemble approach. *Atmospheric Research*, 249, p.105296. [DOI]

Sukoriansky, S., Galperin, B. and Perov, V., 2006. A quasi-normal scale elimination model of turbulence and its application to stably stratified flows. *Nonlinear Processes in Geophysics*, 13(1), pp.9-22. [DOI]

Tao, H., Xing, J., Zhou, H., Pleim, J., Ran, L., Chang, X., Wang, S., Chen, F., Zheng, H. and Li, J., 2020. Impacts of improved modeling resolution on the simulation of meteorology, air quality, and human exposure to PM2.5, O3 in Beijing, China. *Journal of Cleaner Production*, 243, p.118574. [DOI]

Taşpınar, F., 2015. Improving artificial neural network model predictions of daily average PM10 concentrations by applying principle component analysis and implementing seasonal models. *Journal of the Air and Waste Management Association*, 65(7), pp.800-809. [DOI]

Tebal, N. and Pinang, P., 2011. Comparison between multiple linear regression and feed forward back propagation neural network models for predicting PM10 concentration level based on gaseous and meteorological parameters. *Clean Air Research*, 1(4), pp.42-49.

UNECA and UNECE, 2014. Morocco environmental performance reviews. In: *The United Nations*. pp.1-150.

Wang, P., Qiao, X. and Zhang, H., 2020. Modeling PM2.5 and O3 with aerosol feedbacks using WRF/Chem over the Sichuan Basin, southwestern China. *Chemosphere*, 254, p.126735. [DOI]

Wang, Q. and Li, X., 2022. Correlation analysis between meteorological factors and pollutants based on copula theory. *Journal of Physics: Conference Series*, 2168(1), p.012028. [DOI]

Wang, W., Lu, W., Wang, X. and Leung, A.Y.T., 2003. Prediction of maximum daily ozone level using combined neural network and statistical characteristics. *Environment International*, 29(5), pp.555-562. [DOI]

Wang, Y., Yuan, Q., Li, T., Zhu, L. and Zhang, L., 2021. Estimating daily full-coverage near surface O3, CO, and NO2 concentrations at a high spatial resolution over China based on S5P-TROPOMI and GEOS-FP. *ISPRS Journal of Photogrammetry and Remote Sensing*, 175, pp.311-325. [DOI]

World Health Organization, 2006. Health risks of particulate matter from long-range transboundary air pollution. *WHO Regional Office for Europe*, pp.1-89.

Yorkor, B. and Leton, T., 2017. Prediction and modeling of seasonal concentrations of air pollutants in semi-urban region employing artificial neural. *Journal of Environmental Science and Technology*, 10(4), pp.180-192.

Yu, E., Bai, R., Chen, X. and Shao, L., 2022. Impact of physical parameterizations on wind simulation with WRF V3.9.1.1 under stable conditions at planetary boundary layer gray-zone resolution: a case study over the coastal regions of North China. *Geoscientific Model Development*, 15(21), pp.8111-8134. [DOI]